Contribution from the Department of Chemistry,
The University of North Carolina, Chapel Hill, North Carolina 27514

Synthetic and Mechanistic Investigations of the Reductive Electrochemical Polymerization of Vinyl-Containing Complexes of Iron(II), Ruthenium(II), and Osmium(II)

JEFFREY M. CALVERT, RUSSELL H. SCHMEHL, B. PATRICK SULLIVAN, JOHN S. FACCI,
THOMAS J. MEYER,* and ROYCE W. MURRAY*

Received June 4, 1982

The reductive electrochemical polymerizations of 28 vinyl-containing poly(pyridyl) complexes of iron(II), ruthenium(II), and osmium(II) have been investigated. With use of a semiquantitative procedure to establish relative rates of polymer film formation on the electrode, the complexes have been studied with regard to such variables as the number of vinyl ligands and the negative potential limit in the cyclical scan used for electropolymerization. The first step in the electrochemical polymerization involves formation of a ligand-based radical anion, which appears to be the initiator. The possible ensuing reactions are discussed.

Introduction

A considerable background literature has appeared dealing with insoluble, electroactive polymer coatings on a variety of electrode materials.[1-17] A basis for much of the work is the recognition of the resulting potential applications in heterogeneous catalysis, solar energy conversion, directed charge transfer, trace analysis, electrochromics, and potentiometric sensing devices.

We have recently introduced chemical procedures for the preparation of electroactive polymer films based on the reductive electrochemical polymerization of 4-vinylpyridine and vinyl-2,2′-bipyridine complexes of iron(II) and ruthenium(II).[10a-d,12a,c,d,f] Polymeric films of these complexes are electroactive, stable, and reasonably uniform[12a] and can be prepared as homopolymer, copolymer, or spatially segregated bilayer coatings. A distinctive characteristic of the films is that they contain, by their nature, a redox center in each repeating unit of the polymer—a property difficult to achieve in polymer films containing redox-active metal complexes prepared by other methods. Another notable property is that the films are redox conductors,[12f] as distinct from other electrochemically polymerized films which cause passivation[18] or which act as electronic conducting polymers.[3] The redox conductivity permits continued growth of the polymer film since the outer boundary of the film can act as an electron-transfer mediator at the film–solution interface.

The objective of the present work was to expand the scope of the metal complex polymerization chemistry and to examine the nature of the reductive polymerization reaction more closely. The results show that polymerization occurs for many other vinyl-containing ligands (e.g. bis(4-pyridyl)ethylene (BPE), substituted stilbazoles, and *N*-(4-pyridyl)acrylamides (see Figure 1)), and for Os(II) complexes as well as Ru(II). We have also ascertained (and describe elsewhere[10g]) that oxidative electrochemical polymerization of complexes of these

(1) (a) Buttry, D. A.; Anson, F. C. *J. Electroanal. Chem. Interfacial Electrochem.* **1981**, *130*, 333–8. (b) Shigehara, K.; Oyama, N.; Anson, F. C. *J. Am. Chem. Soc.* **1981**, *103*, 2552–8. (c) Shigehara, K.; Oyama, N.; Anson, F. C. *Inorg. Chem.* **1981**, *20*, 518–22. (d) Oyama, N.; Anson, F. C. *Anal. Chem.* **1980**, *52*, 1192–8. (e) Anson, F. C. *J. Phys. Chem.* **1980**, *84*, 3336–8. (f) Scott, N. S.; Oyama, N.; Anson, F. C. *J. Electroanal. Chem. Interfacial Electrochem.* **1980**, *110*, 303–10. (g) Oyama, N.; Anson, F. C. *J. Am. Chem. Soc.* **1979**, *101*, 3450–6. (h) Flanagan, J. B.; Margel, S.; Bard, A. J.; Anson, F. C. *Ibid.* **1978**, *100*, 4248–53.

(2) (a) Rubenstein, I.; Bard, A. J. *J. Am. Chem. Soc.* **1981**, *103*, 5007–13. (b) Peerce, P. J.; Bard, A. J. *J. Electroanal. Chem. Interfacial Electrochem.* **1980**, *114*, 89–115. (c) Peerce, P. J.; Bard, A. J. *Ibid.* **1980**, *112*, 97–115. (d) Peerce, P. J.; Bard, A. J. *Ibid.* **1980**, *108*, 121–5. (e) Itaya, K.; Bard, A. J. *Anal. Chem.* **1978**, *50*, 1487–9.

(3) (a) Diaz, A. F.; Crowley, J.; Bargon, J.; Gardini, G. P.; Torrance, J. B. *J. Electroanal. Chem. Interfacial Electrochem.* **1981**, *121*, 355–61. (b) Diaz, A. F.; Clarke, T. C. *Ibid.* **1980**, *111*, 115–7. (c) Diaz, A. F.; Logan, J. A. *Ibid.* **1980**, *111*, 111–4. (d) Diaz, A. F.; Castillo, J. I. *J. Chem. Soc., Chem. Commun.* **1980**, 397–8. (e) Noufi, R.; Tench, D.; Warren, L. F. *J. Electrochem. Soc.* **1980**, *127*, 2310–1.

(4) (a) Doblhofer, K.; Dürr, W. *J. Electrochem. Soc.* **1980**, *127*, 1041–4. (b) Doblhofer, K.; Nölte, D.; Ulstrup, J. *Ber. Bunsenges. Phys. Chem.* **1978**, *82*, 403–8.

(5) (a) Dubois, J.-E.; Lacaze, P.-C.; Pham, M.-C. *J. Electroanal. Chem. Interfacial Electrochem.* **1981**, *117*, 233–41. (b) Volkov, A.; Tourillon, G.; Lacaze, P.-C.; Dubois, J.-E. *Ibid.* **1980**, *115*, 279–91. (c) Pharm, M.-C.; Tourillon, G.; Lacaze, P.-C.; Dubois, J.-E. *Ibid.* **1980**, *111*, 385–90.

(6) Heineman, W. R.; Wieck, H. J.; Yacynych, A. M. *Anal. Chem.* **1980**, *52*, 345–6.

(7) Akahoshi, H.; Toshima, S.; Itaya, K. *J. Phys. Chem.* **1981**, *85*, 818–22.

(8) (a) Kaufman, F. B.; Schroeder, A. H.; Engler, E. M.; Kramer, S. R.; Chambers, J. Q. *J. Am. Chem. Soc.* **1980**, *102*, 483–8. (b) Schroeder, A. H.; Kaufman, F. B. *J. Electroanal. Chem. Interfacial Electrochem.* **1980**, *113*, 209–24. (c) Schroeder, A. H.; Kaufman, F. B.; Patel, V.; Engler, E. M. *Ibid.* **1980**, *113*, 193–208. (d) Kaufman, F. B.; Engler, E. M. *J. Am. Chem. Soc.* **1979**, *101*, 547–9. (e) Chambers, J. Q. *J. Electroanal. Chem. Interfacial Electrochem.* **1981**, *130*, 381–5.

(9) (a) Laviron, E. *J. Electroanal. Chem. Interfacial Electrochem.* **1981**, *122*, 37–44. (b) Degrand, C.; Laviron, E. *Ibid.* **1981**, *117*, 283–93. (c) Laviron, E.; Roullier, L.; Degrand, C. *Ibid.* **1980**, *112*, 11–23. (d) Laviron, E. *Ibid.* **1980**, *112*, 1–9. (e) Laviron, E. *Ibid.* **1979**, *100*, 263–70.

(10) (a) Abruña, H. D.; Calvert, J. M.; Ellis, C. D.; Meyer, T. J.; Murray, R. W.; Murphy, W. R.; Walsh, J. L. "Chemical Modification of Surfaces"; American Chemical Society: Washington, DC, 1982; Adv. Chem. Ser. No. 192, p 133. (b) Calvert, J. M.; Sullivan, B. P.; Meyer, T. J. *Ibid.* (c) Ellis, C. D.; Murphy, W. R.; Meyer, T. J. *J. Am. Chem. Soc.* **1981**, *103*, 7480–3. (d) Abruña, H. D.; Denisevich, P.; Umana, M.; Meyer, T. J.; Murray, R. W. *Ibid.* **1981**, *103*, 1–5. (e) Calvert, J. M.; Meyer, T. J. *Inorg. Chem.* **1981**, *20*, 27–33. (f) Samuels, G. J.; Meyer, T. J. *J. Am. Chem. Soc.* **1981**, *103*, 307–12. (g) Ellis, C. D.; Margerum, L. D.; Murray, R. W.; Meyer, T. J. *Inorg. Chem.*, in press.

(11) (a) Fukui, M.; Kitani, A.; Degrand, C.; Miller, L. L. *J. Am. Chem. Soc.* **1982**, *104*, 28–33. (b) Degrand, C.; Miller, L. L. *J. Electroanal. Chem. Interfacial Electrochem.* **1981**, *117*, 267–81. (c) Kerr, J. B.; Miller, L. L.; Van de Mark, M. R. *J. Am. Chem. Soc.* **1980**, *102*, 3383–90. (d) Miller, L. L.; Van de Mark, M. R. *J. Electroanal. Chem. Interfacial Electrochem.* **1978**, *88*, 437–40.

(12) (a) Ikeda, T.; Schmehl, R.; Denisevich, P.; Willman, K.; Murray, R. W. *J. Am. Chem. Soc.* **1982**, *104*, 2683. (b) Willman, K. W.; Murray, R. W. *J. Electroanal. Chem. Interfacial Electrochem.* **1982**, *133*, 211. (c) Denisevich, P.; Abruña, H. D.; Leidner, C. R.; Meyer, T. J.; Murray, R. W. *Inorg. Chem.* **1982**, *21*, 2153–61. (d) Ikeda, T.; Leidner, C. R.; Murray, R. W. *J. Am. Chem. Soc.* **1981**, *103*, 7422–5. (e) Facci, J.; Murray, R. W. *J. Electroanal. Chem. Interfacial Electrochem.* **1981**, *124*, 339–43. (f) Denisevich, P.; Willman, K. W.; Murray, R. W. *J. Am. Chem. Soc.* **1981**, *103*, 4727–37. (g) Rolison, D. R.; Umaña, M.; Burgmayer, P.; Murray, R. W. *Inorg. Chem.* **1981**, *20*, 2996–3002. (h) Daum, P.; Murray, R. W. *J. Phys. Chem.* **1981**, *85*, 1225–31. (i) Murray, R. W. *Acc. Chem. Res.* **1980**, *13*, 135–41.

(13) Ellis, D.; Eckhoff, M.; Neff, V. D. *J. Phys. Chem.* **1981**, *85*, 1225–31.

(14) Oyama, N.; Sato, K.; Matsuda, H. *J. Electroanal. Chem. Interfacial Electrochem.* **1980**, *115*, 149–55.

(15) (a) Andrieux, C. P.; Dumas-Bouchiat, J. M.; Saveant, J. M. *J. Electroanal. Chem. Interfacial Electrochem.* **1980**, *114*, 159–63. (b) Andrieux, C. P.; Saveant, J. M. *Ibid.* **1980**, *113*, 139–49.

(16) (a) Haas, O.; Kriens, M.; Vos, J. G. *J. Am. Chem. Soc.* **1981**, *103*, 1318–9. (b) Haas, O.; Vos, J. G. *J. Electroanal. Chem. Interfacial Electrochem.* **1980**, *113*, 139–49.

(17) Bruce, J. A.; Wrighton, M. S. *J. Am. Chem. Soc.* **1982**, *104*, 74–82.

(18) (a) Mengoli, G. *Adv. Polym. Sci.* **1979**, *33*, 1–33. (b) Subramanian, R. V. *Ibid.* **1979**, *33*, 33–58.

0020-1669/83/1322-2151$01.50/0

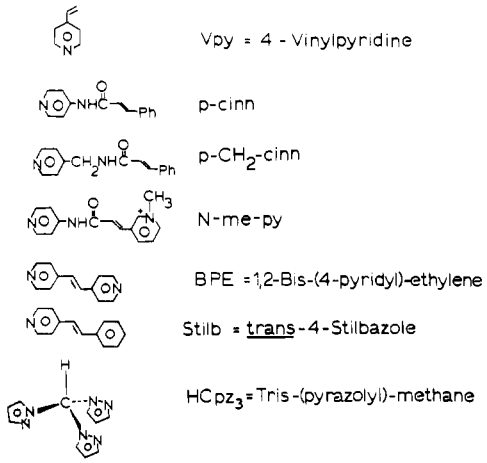

Figure 1. Selected ligands of the polymerizable complexes.

metals is possible with other appropriately substituted ligands. The new series of polymers expands the range of available film redox potentials. In addition, from variations in polymerization rates as a function of structural changes, we have been able to infer certain details of the polymerization mechanism(s).

Experimental Section

Chemicals and Solvents. Water was doubly distilled from alkaline $KMnO_4$. Acetonitrile (Burdick and Jackson) and dichloromethane (Fisher) for electrochemical measurements were stored over Davison 3-Å molecular sieves for at least 24 h before use. CD_3CN and $CDCl_3$ (Aldrich) were the solvents in the ^1H NMR experiments, and tetramethylsilane (Aldrich) provided the reference signal. Tetra-*n*-ethylammonium perchlorate (TEAP) was prepared from the corresponding bromide salt (Eastman) by a previously published procedure.[19] Electrochemical solutions were acetonitrile 0.1 M in TEAP. Other materials except as below were reagent grade and used as received.

The following vinyl-containing ligands were employed in synthesis of ruthenium and osmium complexes: 4-Vinylpyridine (vpy, Aldrich) was distilled at reduced pressure (77 °C, 31 torr) and stored tightly capped in a freeze. Bis(4-pyridyl)ethylene (BPE) was used as received from Aldrich. The ligands *trans*-4-stilbazole (stilb) and various 4′-substituted 4-stilbazoles were generously provided by Professor D. G. Whitten and have been described previously.[20] (The substituted stilbazole ligands will be abbreviated as "4′-X-stilb", X being the functional group Cl, OCH_3, or CN.) Ligands in which the vinyl group is more remote from the metal coordinating site (see Figure 1) were prepared as described next.

***N*-(4-Pyridyl)cinnamamide (*p*-cinn).** Cinnamoyl chloride (2.1 g, 14 mmol) was added to 4-aminopyridine (1.28 g, 14 mmol) dissolved in 20 mL of pyridine, causing rapid formation of a precipitate. The solution was heated to 50 °C and stirred overnight and then poured into a beaker containing 50 mL of cold water and 5 mL of 10% NaOH. The resulting solid was collected and recrystallized from 1:1 water/ethanol: yield 50%; NMR δ 8.3 (doublet, 2), 7.4 (multiplet, 8), 6.7 (doublet, 1).

***N*-(4-Pyridylmethyl)cinnamamide (*p*-CH_2-cinn).** Prepared in a manner similar to that for *p*-cinn: yield 25%; melting range 94–96 °C; NMR δ 8.3 (doublet, 2), 7.9 (multiplet, 1), 7.3 (multiplet, 9), 6.5 (doublet, 1), 4.4 (doublet, 2).

***N*-(3-Pyridyl)cinnamamide (*m*-cinn).** Prepared in a manner similar to that for *p*-cinn: yield 30%; melting range 175–178 °C; NMR δ 8.4 (doublet, 2), 7.9 (multiplet, 2), 7.15 (multiplet, 7), 6.35 (doublet, 2).

***N*-(4-Pyridyl)fumaramide (*p*-fum).** Fumaric acid, ethyl ester (303 mg, 2.1 mmol), was added to 4-aminopyridine (197 mg, 2.1 mmol) dissolved in 50 mL of CH_3CN containing dicyclohexylcarbodiimide (DCC, 433 mg, 2.1 mmol). The mixture was stirred for 4 h and filtered to remove dicyclohexylurea. The filtrate was evaporated to near dryness and the collected precipitate recrystallized from CH_3CN: yield 20%; melting range 158–162 °C; NMR δ 9.25 (multiplet, 1), 8.5 (doublet, 2), 7.6 (multiplet, 2), 7.05 (doublet, 2), 4.25 (quartet, 2), 1.3 (triplet, 3).

***N*-(4-Pyridyl)-β-(3-*N*-methylpyridyl)acrylamide Hexafluorophosphate (*N*-Me-py).** (a) β-(3-Pyridyl)acrylic acid (3 g, 20 mmol) was added to 200 mL of CH_3CN, the mixture heated to boiling, excess CH_3I (15 mL) added, and the stirred mixture heated for 15 h at 40 °C. The solid resulting from the cooled solution was removed by filtration and the iodide salt redissolved in water and reprecipitated by addition of a saturated, aqueous $NaPF_6$ solution. After cooling, the mixture was filtered to remove the white, crystalline product; yield 94%. (b) The β-(3-*N*-methylpyridyl)acrylic acid formed in (a) (5.8 g, 18.8 mmol) was dissolved in 100 mL of CH_3CN, stoichiometric quantities of 4-aminopyridine (1.77 g) and DCC (3.88 g) were added, and the solution was stirred for 4 h. The solution was filtered and evaporated to minimum volume and the resulting precipitate collected and recrystallized from methanol: yield 70%; mp 210 °C dec; NMR (CD_3CN) δ 8.3 (multiplet, 6), 7.6 (multiplet, 2), 7.25 (doublet, 2), 6.55 (doublet, 1), 4.05 (singlet, 3).

Preparations of the metal complexes *cis*-$[Ru(bpy)_2(vpy)_2](PF_6)_2$[10d,21,22] (bpy = 2,2′-bipyridine), *cis*-$[Ru(bpy)_2(vpy)Cl]PF_6$,[10d,21] *cis*-$[Ru(bpy)_2(stilb)_2](PF_6)$[22,23] (stilb = *trans*-4-stilbazole), and *cis*-$[Ru(bpy)_2(BPE)_2](PF_6)$[22,24] (BPE = 1,2-bis-(4-pyridyl)ethylene) were as described in the literature. Syntheses for the remaining complexes are described below.

***cis*-[Ru(phen)$_2$(vpy)$_2$](PF$_6$) (phen = 1,10-Phenanthroline).** To a solution containing 15 mL of EtOH, 15 mL of water, and 0.8 mL (7.5 mmol) of 4-vpy, deoxygenated with N_2 for 20 min, was added 172 mg (0.30 mmol) of $Ru(phen)_2Cl_2 \cdot 2H_2O$.[25] The mixture was heated at reflux under N_2 for 3.5 h and then reduced in volume approximately half by rotary evaporation. Addition of 1 mL of a saturated, aqueous solution of NH_4PF_6 caused immediate precipitation of an orange solid which, after cooling, was filtered, dried, reprecipitated by ether from a minimum volume of acetone, and collected by filtration. The complex was chromatographed on a basic adsorption alumina column with 3:1 (v/v) toluene/acetonitrile mixture as eluant. The solvent was removed from the collected orange fraction, the complex reprecipitated from CH_2Cl_2 by addition to stirring diethyl ether, and the filtered, ether-rinsed yellow-orange solid collected and dried; yield 60%. (Important note: Solutions of this complex and others of the type $Ru(chel)_2(L)_2^{2+}$ (chel = chelating ligand such as bpy; L = pyridyl type ligand) must be protected from light at all times to avoid photosubstitution reactions known for these complexes.[26])

***cis*-[Ru(bpy)$_2$(L)$_2$](PF$_6$)$_2$ (L = 4′-Cl-stilb, 4′-CN-stilb, 4′-OMe-stilb, *p*-cinn, *m*-cinn, *p*-CH$_2$-cinn, *p*-fum).** Preparation of these complexes was similar to that for *cis*-$[Ru(phen)_2(vpy)_2](PF_6)_2$, except that *cis*-$Ru(bpy)_2Cl_2 \cdot 2H_2O$ was employed as starting material and an 8–10-fold stoichiometric excess of ligand was used in place of vpy. Reaction times for the stilbazole derivatives were extended to 18–24 h. Several of the complexes were isolated as perchlorate salts by addition of saturated, aqueous $LiClO_4$. Eluants for chromatography of these materials were somewhat more polar, e.g., 2:1 or 1:1 (v/v) toluene/CH_3CN mixtures. The two linkage isomers of the 4′-CN-stilb complex formed in the reaction mixture in a ratio of approximately 3:1 (pyridine bound:nitrile bound) could not be separated chromatographically. Following chromatography, the complexes were reprecipitated from either CH_3CN or CH_2Cl_2 into ether. Solutions of these complexes must be protected from light. Yields: L = 4′-Cl-stilb (81%), 4′-CN-stilb, both isomers (85%), 4′-OMe-stilb (37%), *p*-cinn

(19) Sawyer, D. T.; Roberts, J. L. "Experimental Electrochemistry for Chemists"; Wiley-Interscience: New York, 1974; p 212.
(20) Wildes, P. D. Ph.D. Dissertation, The University of North Carolina, Chapel Hill, NC, 1970.
(21) A sample of the complex was generously provided by Mr. W. R. Murphy.
(22) This complex can be prepared via the procedure described for $[Ru(phen)_2(vpy)_2](PF_6)_2$, with $Ru(bpy)_2Cl_2 \cdot 2H_2O$ as the starting material.
(23) A sample of this complex was generously provided by Professor David G. Whitten. See: Zarnegar, P. P.; Whitten, D. G. *J. Am. Chem. Soc.* **1971**, *93*, 3776–7.
(24) A previously prepared sample, synthesized by another method and repurified by chromatographic methods described in this paper was used. See: Powers, M. J.; Callahan, R. W.; Salmon, D. J.; Meyer, T. J. *Inorg. Chem.* **1976**, *15*, 894–900.
(25) This complex was prepared in a manner identical with that reported for the bipyridine analogue in: Sullivan, B. P.; Salmon, D. J.; Meyer, T. J. *Inorg. Chem.* **1978**, *17*, 3334–41.
(26) Durham, B.; Walsh, J. L.; Carter, C. L.; Meyer, T. J. *Inorg. Chem.* **1980**, *19*, 860–5.

(54%), *m*-cinn (38%), *p*-CH_2-cinn (50%), *p*-fum (30%).

***mer*-[Ru(trpy)(vpy)$_3$](PF$_6$)$_2$ (trpy = 2,2′,2″-Terpyridine).** To a solution containing 100 mL of water, 100 mL of ethanol, and 3.2 mL (30 mmol) of 4-vinylpyridine was added Ru(trpy)Cl_3 (440 mg, 1.0 mmol),[27] and the mixture was heated at reflux for 24 h. The solvent volume was reduced by rotary evaporation to approximately half of the original volume, aqueous NH_4PF_6 added, and after cooling, the resulting brown precipitate filtered and dried. The solid was extracted with CH_2Cl_2, the solution reduced to minimum volume, and the solid reprecipitated by addition of ether. The complex was chromatographed with first CH_2Cl_2 and then CH_3OH/CH_2Cl_2 as eluants. The product was then isolated by reprecipitation from CH_2Cl_2 with ether, filtered, rinsed with ether, and dried; yield 54%.

***mer*-[Ru(trpy)(L)$_3$](PF$_6$)$_2$ (L = BPE, stilb, 4′-Cl-stilb).** These materials were prepared and purified in a manner similar to that for the vpy complex, with the exception that a 9-fold excess of the appropriate ligand was used in place of vpy in the reflux step and the chromatographic eluant was 2:1 toluene/CH_3CN. The desired complexes were orange-brown and were the last major band to be eluted. Yields: L = BPE (52%), stilb (16%), 4′-Cl-stilb (46%).

[Ru(trpy)(stilb)$_2$Cl]PF$_6$. This red-brown solid was isolated as a side product during chromatographic purification of Ru(trpy)(stilb)$_3^{2+}$ (see above), eluting from the column just prior to the tris(stilbazole) complex; yield 19%.

***fac*-[Ru(HC(pz)$_3$)(vpy)$_3$](PF$_6$)$_2$ ((HC(pz)$_3$) = Tripyrazolylmethane).** To a well-deoxygenated solution containing 150 mL of water, 150 mL of ethanol, and 5 mL of 4-vinylpyridine was added Ru(HC(pz)$_3$)Cl_3 (503 mg, 1.19 mmol).[28] The mixture was heated at reflux under N_2 for 7 h and reduced by rotary evaporation to about half the original volume, 1 mL of saturated NH_4PF_6 solution was added, and after cooling, the resulting green precipitate was collected by filtration. The solid was dissolved in CH_2Cl_2, leaving an insoluble (polymeric?) material, and then precipitated from ether and filtered. In the chromatography used to isolate the complex from the crude mixture of seven products, 3:1 toluene/CH_3CN rapidly eluted a flesh-colored band; the remaining fractions were removed with neat CH_3CN, leaving behind an insoluble green (likely thermal polymerization) product at the top of the alumina column. After concentration, the combined fractions were eluted slowly from a fresh column with 4:1 toluene/CH_3CN. The last (yellow-green) band was collected, the solvent removed, the complex reprecipitated from CH_2Cl_2 with ether, and the pale green solid washed with ether and dried; yield 40%.

[Ru(trpy)(bpy)Cl]PF$_6$. Ru(trpy)Cl_3 (528 mg, 1.20 mmol) and bpy (197 mg, 1.26 mmol) in 150 mL of 4:1 (v/v) water/ethanol were heated at reflux for 5 h, excess solid LiCl was added, and the mixture was heated for an additional 30 min. NH_4PF_6 was added, the solution volume reduced by rotary evaporation to about 50 mL, and a brown solid was precipitated from the cooled solution, which was redissolved in acetone and precipitated from ether. The complex was chromatographed with use of 2:1 toluene/CH_3CN and the complex precipitated from a small volume of the red-brown fraction dissolved in acetone by addition to ether; yield 49%.

[Ru(trpy)(bpy)(vpy)](ClO$_4$)$_2$. To a solution containing 25 mL of water, 25 mL of ethanol, and 0.2 mL (2 mmol) of 4-vinylpyridine was added [Ru(trpy)(bpy)Cl]ClO_4 (100 mg, 0.16 mmol) and the mixture heated at reflux for 5 h. After the reaction solvent volume was reduced by half by rotary evaporation, an aqueous solution saturated in NH_4PF_6 was added and a brown precipitate collected from the cooled solution. The complex was chromatographed with 2:1 toluene/CH_3CN as eluant and then reprecipitated from acetone by addition to ether; yield 85%.

[Ru(trpy)(bpy)(L)](PF$_6$)$_2$ (L = BPE, 4′-Cl-stilb). These materials were prepared and purified in a similar manner to the vpy complex except that a 4-fold excess of the ligand L was used in place of vpy in the reflux step. Yields: L = BPE (70%), 4′-Cl-stilb (76%).

***cis*-[Ru(bpy)$_2$(*N*-Me-py)$_2$](PF$_6$)$_4$.** Ru(bpy)$_2Cl_2$·$2H_2O$ (100 mg, 0.21 mmol) was dissolved in an N_2-deoxygenated 1:1 water/ethanol solution containing LiCl (52 mg, 1.24 mmol), the ligand, *N*-Me-py (800 mg, 2.1 mmol), added, and the solution heated at reflux under N_2 for 5 h. The cooled solution was filtered, the solvent reduced in volume by about half, and the solution cooled in ice for 30 min and then refiltered. An orange precipitate was obtained by adding aqueous $NaPF_6$ to the filtrate, which was dried and then chromatographed with CH_3CN. The monosubstituted complex and excess free ligand were eluted first; the disubstituted complex was subsequently eluted with 5% CH_3OH/CH_3CN. This complex was recrystallized from CH_3CN added to ether; yield 20%.

***cis*-[Ru(*i*-Pr-bpy)$_2$(*p*-cinn)$_2$](PF$_6$)$_2$ (*i*-Pr-bpy = 2,2′-Bipyridine-4,4′-dicarboxylic Acid, Diisopropyl Ester).** Ru(*i*-Pr-bpy)$_2Cl_2$ (85 mg, 0.1 mmol) in N_2-deaerated, 1:1 water/ethanol solution containing *p*-cinn ligand (224 mg, 1 mmol) was heated at reflux for 7 h. The solution was evaporated to a small volume and filtered to remove excess ligand, and the complex was precipitated by addition of aqueous $NaPF_6$ and purified by chromatography with neat CH_3CN eluant. The red-orange fraction was evaporated to dryness and the complex recrystallized from CH_3CN added to ether; yield 30%.

***N*-(*p*-Ferrocenylphenyl)-β-(3-*N*-methylpyridyl)acrylamide Hexafluorophosphate (Ferrocene Derivative).** Stoichiometric amounts of 4-aminophenylferrocene (100 mg, 0.36 mmol), β-(3-*N*-methylpyridyl)acrylic acid (111 mg), and DCC (75 mg) were stirred in 15 mL of CH_3CN at room temperature for 5 h in the dark, and the solution was filtered and evaporated to dryness. The product was dissolved in CH_2Cl_2, the solution extracted with 10% aqueous NaOH to remove excess acid and reduced to a small volume, and the red precipitate collected by filtration; yield 25%.

***cis*-[Os(bpy)$_2$(vpy)$_2$](PF$_6$)$_2$.** A deoxygenated suspension of *cis*-Os(bpy)$_2(CO_3)$·$2H_2O$[30] (240 mg, 0.40 mmol) in 25 mL of *n*-butanol plus 0.11 mL (1.0 mmol) of CF_3CO_2H was gently heated with stirring for 30 min, then excess vpy (1 mL) added, and the reaction heated at reflux for 4 h. The cooled contents of the flask were added to 100 mL of water containing excess NH_4PF_6, and the flocculent precipitate was collected. Chromatography yielded a dark green band, which eluted with 1:1 toluene/CH_3CN. The complex was reprecipitated from CH_2Cl_2 into ether, filtered, and dried; yield 30%. An original sample of this material was kindly supplied by Dr. E. M. Kober.

***cis*-[Os(bpy)$_2$(*p*-cinn)$_2$](PF$_6$).** This complex was prepared like the above osmium (vpy)$_2$ complex except that a 10-fold excess of the *p*-cinn ligand was used; yield 60%.

***cis*-[Os(bpy)$_2$(L)Cl](PF$_6$) (L = vpy or BPE).** To an N_2-deoxygenated suspension of *cis*-Os(bpy)$_2Cl_2$·H_2O[31] (250 mg, 0.42 mmol) in 50 mL of 1:1 water/ethanol was added excess ligand, vpy (1 mL, 9 mmol) or BPE (500 mg, 2.75 mmol), and the mixture heated at reflux for 20 h. The solution plus 100 mL of water was reduced to about half the original volume, filtered into a separatory funnel and extracted with four 50-mL portions of ether. To the aqueous layer was added aqueous NH_4PF_6 and the flocculent precipitate filtered, washed with water and ether, and dried. The solid was purified by chromatography with 1:1 toluene/CH_3CN as eluant. The first (purple-brown) band was collected, the solvent removed, and the complex isolated by reprecipitation from CH_2Cl_2 into ether. Yields: L = vpy(80%), BPE (50%).

Electrodes and Instrumentation. Teflon-shrouded platinum-disk electrodes were mechanically polished before each experiment with 1-μm diamond paste (Buehler). A disposable, 20-mL scintillation vial served as a convenient, one-compartment electrochemical cell. Electrochemical instrumentation included a PAR Model 174A polarographic analyzer and a home-built waveform generator.[32] Measurements are referenced to a NaCl-saturated calomel electrode (SSCE) at 25 ± 2 °C and are uncorrected for junction potential effects. No *iR* compensation was employed. A platinum wire served as auxiliary electrode.

^1H NMR spectra of the new polymerizable ligands were recorded in $CDCl_3$ or CD_3CN with a Perkin-Elmer R24B spectrometer, and variable-angle XPS measurements were made on a PHI Model 548 electron spectrometer. Elemental analyses were performed by either Integral Microanalytical Laboratories, Raleigh, NC, or by Galbraith Laboratories, Knoxville, TN.

(27) Sullivan, B. P.; Calvert, J. M.; Meyer, T. J. *Inorg. Chem.* **1980**, *19*, 1404–7.
(28) This complex was prepared by a reaction scheme analogous to that used for *mer*-Ru(trpy)Cl_3 cited in ref 26. A sample of this material was generously provided by Dr. M. S. Thompson.
(29) Sprintschnik, G. H. W.; Kirsch, P. P.; Whitten, D. G. *J. Am. Chem. Soc.* **1977**, *99*, 4947–8.
(30) Kober, E. M.; Caspar, J. V.; Sullivan, B. P.; Meyer, T. J., manuscript in preparation.
(31) Buckingham, D. A.; Dwyer, F. P.; Goodwin, H. A.; Sargeson, A. M. *J. Am. Chem. Soc.* **1964**, *17*, 325–36.
(32) Woodward, W. S.; Rocklin, R. D.; Murray, R. W. *Chem., Biomed. Environ. Instrum.* **1979**, *9*, 95–105.

Procedure for Electropolymerization Experiments. Concentrations of electropolymerizable complexes of 1–3 mM were used, normalizing for the number of polymerizable groups by using for complexes containing three polymerizable groups, [complex] ≈ 1 mM, for two groups, [complex] ≈ 1–2 mM, and for one group, [complex] ≈ 2–3 mM. Solutions were deoxygenated with CH_3CN-saturated nitrogen, and those containing bis chelate complexes were protected from light to avoid photosubstitution.

The electropolymerization was carried out by scanning the Pt-disk potential repeatedly ca. 150 mV past (more negative than) $E_{1/2}$ for the reduction wave of interest. When the anodic component of the wave was not well-defined, the negative limit was set at about 100 mV past $E_{p,c}$.[33] The positive limit of the cyclic potential scan was chosen between −0.5 and −1.0 V. The number of scans required to generate a particular quantity of polymer film depended on the reactivity and concentration of the monomer complex and on the negative potential limit. The potential scan rate was 200 mV/s except as noted.

After formation of the polymer film, the electrode was rinsed with acetone and air-dried and its electrochemical response examined in fresh TEAP/CH_3CN electrolyte. The quantity of electroactive sites in the film (Γ) was determined from the charge under the anodic M(III/II) wave.

Polymerization Efficiency. The efficiency of polymerization, or yield of electroactive polymer film per electron introduced by electrochemical reduction, can be determined by comparing the total cathodic charge passed in the reductive polymerization experiment to the anodic charge for the $M^{3+/2+}$ reaction in the resulting electroactive polymer film. The total cathodic charge, or the amount of monomer that diffused to the electrode and was reduced during film deposition, was estimated directly from experimental voltammograms in some cases and in others indirectly from the size of the corresponding $M^{3+/2+}$ voltammogram of the monomer. The ratio of the anodic to the cathodic charge will be termed Φ_{poly}. Experimental estimates of Φ_{poly} are presented in Table III.

Results and Discussion

Synthesis of New Polymerizable Complexes. The initial experiments on electropolymerization of transition-metal complexes by Abruña et al. dealt with the homopolymerization of *cis*-$Ru(bpy)_2(vpy)_2^{2+}$ [10d] and its copolymerization with $[Ru(bpy)_2(vpy)Cl]^+$. Other complexes subsequently studied have been $[Ru(bpy)_2(vpy)X]^+$ (X = NO_2^-,[12b] N_3^- [10a]) and $[Ru(vbpy)_3]^{2+}$ and $[Fe(vbpy)_3]^{2+}$ [10d,12b,c,e] (vbpy = 4-methyl-4′-vinyl-2,2′-bipyridine). In this paper we have exploited the well-established synthetic chemistry of poly(pyridyl) complexes of the Fe–Ru–Os triad to prepare a large family of new polymerizable monomers. The general synthetic strategy used for Ru(II) and Os(II) complexes was based on substitutional reactions of the dichloride complexes *cis*-$Ru(bpy)_2Cl_2$ and *cis*-$Os(bpy)_2Cl_2$. Ethanol/water mixtures containing the complexes were heated at reflux in the presence of the added ligand. For Ru(II), direct substitution of one or both halide ions can be achieved by varying the reaction time and concentration of vinyl ligand (VL):

$$[cis\text{-}Ru(bpy)_2Cl_2] + VL \xrightarrow[\Delta\ (0.5\text{–}3\ h)]{H_2O/EtOH} [cis\text{-}Ru(bpy)_2(VL)Cl]^+ + Cl^- \quad (1)$$

$$[cis\text{-}Ru(bpy)_2Cl_2] + 2VL \xrightarrow[\Delta\ (1.5\text{–}24\ h)]{H_2O/EtOH} [cis\text{-}Ru(bpy)_2(VL)_2]^{2+} + 2Cl^- \quad (2)$$

$$[cis\text{-}Os(bpy)_2Cl_2] + VL \xrightarrow[\Delta\ (24\ h)]{H_2O/EtOH} [cis\text{-}Os(bpy)_2(VL)Cl]^+ + Cl^- \xrightarrow[\text{long times}]{VL,\ \Delta(\text{days})} [cis\text{-}Os(bpy)_2(VL)_2]^{2+} + \text{polymers} \quad (3)$$

The preferred synthesis of disubstituted Os(II) complexes was based on the carbonato complex $Os(bpy)_2(CO)_3$[30] as a starting material:

$$[Os(bpy)_2(CO_3)] + 2H^+ \xrightarrow{n\text{-BuOH}} [cis\text{-}Os(bpy)_2(n\text{-BuOH})_2]^{2+} + H_2CO_3 \quad (4)$$

$$[cis\text{-}Os(bpy)_2(n\text{-BuOH})_2]^{2+} + 2VL \rightarrow [cis\text{-}Os(bpy)_2(VL)_2]^{2+} + 2\,n\text{-BuOH} \quad (5)$$

Synthesis of terpyridine complexes of Ru(II)-containing vinyl ligands was achieved via the direct reaction between *mer*-$Ru^{III}(trpy)Cl_3$ and excess VL in water/alcohol solutions, which gave both $Ru^{II}(trpy)(VL)_2Cl^+$ and $Ru^{II}(trpy)(VL)_3^{2+}$. The two products were separated by column chromatography. The complexes $Ru(trpy)(VL)_2Cl^+$ probably have the trans geometry, based on the expected facile substitution of the initially formed *cis*-$Ru^{II}(trpy)(L)Cl_2$.[27]

Synthesis of the mixed tripyrazolylmethane/vinylpyridine complex *fac*-$Ru^{II}(HC(pz)_3)(vpy)_3^{2+}$ was accomplished by heating at reflux the corresponding chloro complex and 4-vinylpyridine in water/alcohol solution:

$$[Ru^{III}(HC(pz)_3)Cl_3] + 3vpy \xrightarrow[\Delta\ (7\ h)]{H_2O/EtOH} [Ru^{II}(HC(pz)_3)(vpy)_3]^{2+} + 3Cl^- \quad (6)$$

The reducing equivalents necessary to convert Ru(III) into Ru(II) in eq 6 and in the reaction of $Ru(trpy)Cl_3$ described above apparently come from the ethanol component in the solvent.

Nearly all of the vinyl-containing ligands used in this study either were commercial samples or were synthesized and attached to the metal complexes as intact units. An interesting alternate approach to the synthesis of electropolymerizable monomers was also developed. In this approach a metal complex containing an attached primary amine group was prepared and subsequently allowed to react with a vinyl-containing acid or acid chlorides. Equation 7 illustrates the

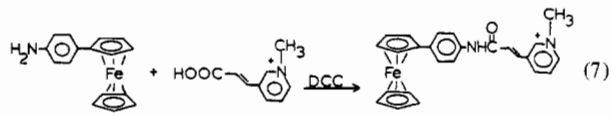
(7)

use of this approach in the synthesis of an electropolymerizable ferrocene derivative. A real advantage to the alternate approach is that the electropolymerizable monomer is synthesized under mild conditions, which minimizes complications arising from ligand polymerization under more forcing conditions.

All new metal complexes were purified by chromatographic techniques developed previously, usually with toluene/acetonitrile mixtures as eluant and alumina as the column support. In general, PF_6^- salts were used to take advantage of their favorable solubility in solvents such as acetonitrile, acetone, and methylene chloride. Elemental analyses obtained for the complexes are listed in Table I.

Solution Cyclic Voltammetry of the Complexes. Table II shows oxidative ($E^{\circ\prime}(ox)_{soln}$) and reductive ($E^{\circ\prime}(red)_{soln}$) formal potentials from the results of cyclic voltammetric experiments in acetonitrile. The M(III/II) potential values for the series vary by 1.1 V depending on ligand and metal, the two extremes being $[Os(bpy)_2(BPE)Cl]^+$ (0.33 V) and $[Ru(i\text{-}Pr\text{-}bpy)_2(p\text{-}cinn)_2]^{2+}$ (1.46 V).

In most cases, the two reductions (which are of primary interest here) correspond to formation of radical anions, as electrons are added to the π^* orbitals of the poly(pyridine) ligands:[34]

$$[Ru^{II}(bpy)_2(VL)_2]^{2+} + e^- \rightleftharpoons [Ru^{II}(bpy)(bpy^{-}\cdot)(VL)_2]^+ \quad (8)$$

$$[Ru^{II}(bpy)(bpy^{-}\cdot)(VL)_2]^+ + e^- \rightleftharpoons [Ru^{II}(bpy^{-}\cdot)_2(VL)_2]^0 \quad (9)$$

(33) Definitions: $E_{p,c}$ = cathodic peak potential; $E_{p,a}$ = anodic peak potential. $\Delta E_p = E_{p,a} - E_{p,c}$. $E^{\circ\prime} = {}^1/_2(E_{p,a} + E_{p,c})$; E_{fwhm} = peak width at half-height.

Table I. Elemental Analyses

compd	calcd			obsd		
	% C	% H	% N	% C	% H	% N
p-cinn·H_2O	69.41	5.83	11.56	70.49	5.84	11.81
p-CH_2-cinn[a]	75.59	5.93	11.76			
m-cinn	74.98	5.39	12.48	75.07	5.47	12.46
N-Me-py·H_2O	41.70	3.99	10.42	41.95	4.09	10.42
p-fum	60.05	5.50	12.72	60.20	5.70	12.66
$[Os(bpy)_2(vpy)_2](PF_6)_2$	47.44	3.15	8.74	46.92	2.91	8.49
$[Os(bpy)_2(vpy)Cl]PF_6$	40.70	3.03	8.38	40.33	2.71	7.92
$[Ru(phen)_2(vpy)_2](PF_6)_2$	41.13	2.94	8.89	40.90	2.41	8.73
$[Ru(trpy)(vpy)_3](PF_6)_2$	45.56	3.33	8.85	45.99	3.33	8.95
$[Ru(trpy)(bpy)(vpy)](ClO_4)_2·4H_2O$	44.14	3.94	9.66	44.69	3.76	9.89
$[Ru(HC(pz)_3)(vpy)_3](PF_6)_2$	40.42	3.40	13.70	39.66	2.91	13.50
$[Ru(trpy)(bpy)(BPE)](PF_6)_2$	46.14	3.04	10.19	46.06	2.64	9.18
$[Ru(trpy)(BPE)_3](PF_6)_2$	52.29	3.53	10.77	49.68	2.81	10.16
$[Os(bpy)_2(BPE)Cl]PF_6$[a]	44.40	3.03	9.72			
$[Ru(trpy)(stilb)_3](PF_6)_2$	55.51	3.80	7.20	55.18	3.38	7.45
$[Ru(trpy)(stilb)_2Cl]PF_6$	56.11	3.79	7.99	55.93	3.38	7.88
$[Ru(trpy)(bpy)(4'\text{-Cl-stilb})](PF_6)_2$	45.80	2.94	8.44	46.53	3.26	8.55
$[Ru(bpy)_2(4'\text{-Cl-stilb})_2](PF_6)_2$	48.67	3.20	7.41	49.29	3.04	7.44
$[Ru(trpy)(4'\text{-Cl-stilb})_3](PF_6)_2$	50.91	3.41	6.60	51.11	2.45	6.70
$[Ru(bpy)_2(4'\text{-OMe-stilb})_2](PF_6)_2$	51.13	3.76	7.47	51.18	3.38	7.45
$[Ru(bpy)_2(4'\text{-CN-stilb})_2](PF_6)_2$[a]	51.64	3.25	10.05			
$[Ru(bpy)_2(p\text{-cinn})_2](PF_6)_2$	49.28	3.62	9.57	49.87	3.67	9.58
$[Os(bpy)_2(p\text{-cinn})_2](PF_6)_2$[a]	45.74	3.36	8.88			
$[Ru(bpy)_2(m\text{-cinn})_2](ClO_4)_2$	74.98	5.39	12.48	75.07	5.47	12.46
$[Ru(i\text{-Pr-bpy})_2(p\text{-cinn})_2](PF_6)_2$[a]	55.79	4.69	6.11			
$[Ru(bpy)_2(p\text{-CH}_2\text{-cinn})_2](ClO_4)_2$	55.13	4.07	10.30			
$[Ru(bpy)_2(p\text{-fum})_2](ClO_4)_2$	60.05	5.50	12.72	60.20	5.70	12.66
$[Ru(bpy)_2(N\text{-Me-py})_2](PF_6)_4$[a]	38.16	3.21	9.28			
ferrocene derivative	51.21	4.26	4.78	49.40	4.04	4.64
$[Ru(trpy)(bpy)Cl]PF_6$	44.73	2.86	10.44	44.57	2.80	10.15

[a] Elemental analyses were not obtained for these compounds or complexes.

Table II. Solution Potentials, Surface Potentials, and Normalized Surface Coverages

complex[a]	$E^{\circ\prime}(ox)_{soln}$[b,c]	$E^{\circ\prime}(ox)_{surf}$[b,d]	$E^{\circ\prime}(red,1)_{soln}$[c,e]	$(\Gamma/\Gamma_0)_1$[g,h]	$E^{\circ\prime}(red,2)_{soln}$[c,f]	$(\Gamma/\Gamma_0)_2$[g,i]
$Ru(trpy)(bpy)(vpy)^{2+}$	1.21	1.20	−1.26	0.02	−1.59	0.13
$Ru(trpy)(bpy)(BPE)^{2+}$	1.21	1.20	−1.26	0.12	−1.58	0.10
$Ru(trpy)(bpy)(4'\text{-Cl-stilb})^{2+}$	1.21	1.20	−1.35	0.005	−1.55	0.035
$Ru(bpy)_2(vpy)Cl^+$	0.76	0.77	−1.50	0.019[j]		
$Os(bpy)_2(vpy)Cl^+$	0.36	1.35	−1.46	0.28		
$Os(bpy)_2(BPE)Cl^+$	0.33	0.33	−1.50	0.15		
ferrocene derivative	0.40	0.41	−1.07[k]	5–10		
$Ru(bpy)_2(vpy)_2^{2+}$	1.25	1.22	−1.36	1.0	−1.54	3.7
$Os(bpy)_2(vpy)_2^{2+}$	0.77	1.74	−1.33	3.5	−1.53	38
$Ru(bpy)_2(BPE)_2^{2+}$	1.30	1.23	−1.35	0.40–0.58	−1.53	0.34–0.83
$Ru(bpy)_2(stilb)_2^{2+}$	1.23	1.22	−1.36	0.04	−1.54	2.6
$Ru(bpy)_2(4'\text{-Cl-stilb})_2^{2+}$	1.22	1.24	−1.38	0.24	−1.54	5.3
$Ru(bpy)_2(4'\text{-OMe-stilb})_2^{2+}$	1.19[l]	1.25[m]	−1.39	0.0007	−1.59	0.21–0.58
$Ru(bpy)_2(4'\text{-CN-stilb})_2^{2+}$	1.25[n]	1.23[n]	−1.40	0.95[o]	−1.64	0.32–0.37[o]
$Ru(bpy)_2(p\text{-cinn})_2^{2+}$	1.19	1.20	−1.39		−1.70	75
$Os(bpy)_2(p\text{-cinn})_2^{2+}$	0.74	0.72	−1.36		−1.65	65
$Ru(bpy)_2(m\text{-cinn})^{2+}$	1.28	1.27	−1.38		−1.63	24
$Ru(bpy)_2(p\text{-CH}_2\text{-cinn})_2^{2+}$	1.26		−1.39	~0	−1.61	~0
$Ru(bpy)_2(p\text{-fum})_2^{2+}$	1.22	1.20	−1.40		−1.71	60
$Ru(bpy)_2(N\text{-Me-py})_2^{4+}$	1.22	1.19	−1.39[p]	40	−1.65	
$Ru(phen)_2(vpy)_2^{2+}$	1.25	1.24	−1.37	0.4	−1.51	20
$Ru(trpy)(stilb)_2Cl^+$	0.77	0.78	−1.38	0.005	−1.74[k]	8–33
$Ru(i\text{-Pr-bpy})_2(p\text{-cinn})_2^{2+}$	1.46		−0.96	~0	−1.16	~0
$Ru(trpy)(vpy)_3^{2+}$	1.23	1.22	−1.24	3.9–5.3	−1.76[k]	52–164
$Ru(trpy)(BPE)_3^{2+}$	1.23	1.30	−1.26	5.6–6.6	−1.54[k]	120–164
$Ru(trpy)(stilb)_3^{2+}$	1.20	1.23	−1.25	0.004	−1.68[k]	17–45
$Ru(trpy)(4'\text{-Cl-stilb})_3^{2+}$	1.20	1.22	−1.25	0.03–0.06	−1.60[k]	125–269
$Ru(HC(pz)_3)(vpy)_3^{2+}$	1.17	1.16	−1.58	2.4–220		

[a] Electrolyte was 0.1 M TEAP/CH_3CN. All potentials are reported in volts vs. SSCE. [b] M(III/II) couple; metal oxidation. [c] Value for complex in solution. [d] Value for surface-bound complex. [e] First ligand-localized reduction. [f] Second ligand-localized reduction. [g] Surface coverages of complex obtained, relative to that produced by cycling through the first reduction of $Ru(bpy)_2(vpy)_2^{2+}$. Normalized for concentration of complex in solution and number of scans. [h] Cycled through first reduction only. [i] Cycled through both reductions. [j] Total of all electroactive material; includes both chloro and acetonitrile complexes (see text). [k] Reduction irreversible; value of $E_{p,c}$. [l] Irreversible oxidation of methoxystilbazole group at $E_{p,a} = 1.47$ V. [m] Irreversible oxidation of methoxystilbazole group at $E_{p,a} = 1.57$ V. [n] Potential for pyridine-bound isomer. [o] Calculated from corrected solution concentration of pyridine-bound isomer. [p] Also, irreversible reduction of *N*-Me-py group at $E_{p,c} = -1.0$ V.

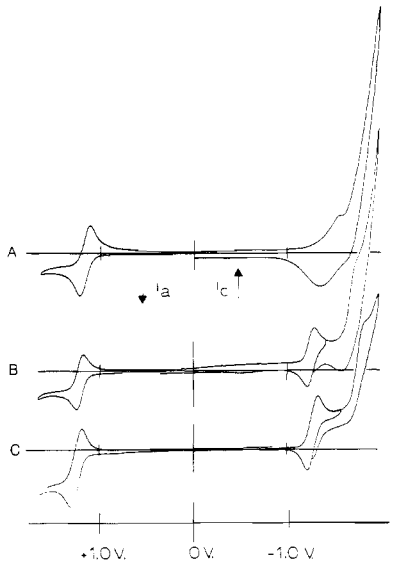

Figure 2. Solution cyclic voltammograms showing $Ru^{III/II}$ couples (+1.2 V), $trpy^{0/-}$ couples (−1.24 V), and direct, irreversible pyridine- or vinylpyridine-localized reductions: (A) *fac*-$[Ru(HC(pz)_3)(vpy)_3]^{2+}$; (B) *mer*-$[Ru(trpy)(vpy)_3]^{2+}$; (C) *mer*-$[Ru(trpy)(py)_3]^{2+}$. The concentration of complex was $\sim 5 \times 10^{-4}$ M. The scans were initially in the oxidative direction beginning at 0 V.

A similar pattern is observed for the mixed terpyridine/bipyridine complexes, although here the first reduction is apparently at π^* orbitals mainly trpy in character:

$$[Ru^{II}(trpy)(bpy)(VL)_2]^{2+} + e^- \rightleftharpoons [Ru^{II}(trpy^-\cdot)(bpy)(VL)]^+ \quad (10)$$

$$[Ru^{II}(trpy^-\cdot)(bpy)(VL)]^+ + e^- \rightleftharpoons [Ru^{II}(trpy^-\cdot)(bpy^-\cdot)(VL)]^0 \quad (11)$$

The suggestion of a trpy-based initial reduction is supported by a comparison of the MLCT transition energies in the visible spectra of Ru^{II}–bpy and –trpy VL-containing complexes, from which it seems clear that the lowest π^* levels are in the order trpy < bpy.[35] It was not possible to observe a third (and presumably VL-localized) reduction for either the VL or $(VL)_2$ complexes, and these processes apparently occur at potentials beyond −2.0 V.

In some cases direct reduction of the vinyl-containing ligand was observed. For the complexes $[Ru(trpy)(VL)_3]^{2+}$, the first reduction appears to be at the trpy ligand and the second at the VP ligand as shown in eq 12 and 13. Figure 2 shows cyclic

$$[Ru^{II}(trpy)(VL)_3]^{2+} + e^- \rightleftharpoons [Ru^{II}(trpy^-\cdot)(VL)_3]^+ \quad (12)$$

$$[Ru^{II}(trpy^-\cdot)(VL)_3]^+ + e^- \rightleftharpoons [Ru^{II}(trpy^-\cdot)(VL^-\cdot)(VL)_2] \quad (13)$$

voltammograms for $[Ru(trpy)(py)_3]^{2+}$ and $[Ru(trpy)(vpy)_3]^{2+}$. In the former complex, the pyridine-localized reduction is evident at $E_{p,c} = -1.96$ V, a potential comparable to that observed for $[Ru(py)_6]^{2+}$ ($E_{p,c} = -1.93$ V).[36] By analogy, the irreversible reduction of $[Ru(trpy)(vpy)_3]^{2+}$ at $E_{p,c} = -1.76$ V is presumably assignable to the $vpy^{0/-}$ couple. The small positive shift in potential is consistent with the electron-withdrawing character of the vinyl substituent. Accessibility of a VL-localized reduction at relatively positive potentials has important consequences with regard to the polymerizability of the trpy complexes and is discussed later.

(34) (a) Anderson, C. P.; Salmon, D. J.; Meyer, T. J.; Young, R. C. *J. Am. Chem. Soc.* **1977**, *99*, 1980–2. (b) Creutz, C.; Sutin, N. *Ibid.* **1976**, *98*, 6384–5.
(35) Calvert, J. M.; Meyer, T. J., unpublished results.
(36) For preparation and oxidative electrochemistry of this complex, see: Templeton, J. L. *J. Am. Chem. Soc.* **1979**, *101*, 4906–17.

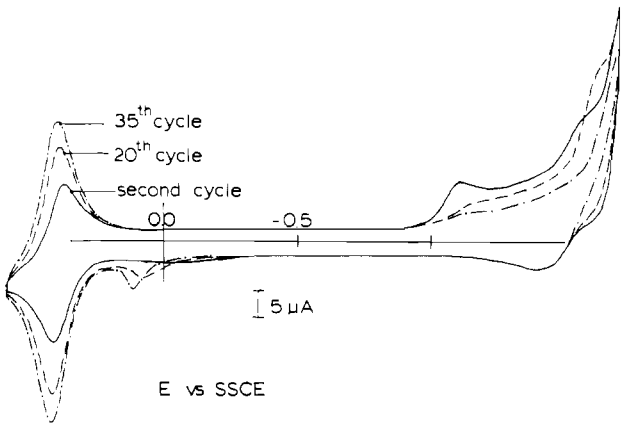

Figure 3. Polymerization of the ferrocene derivative in 0.1 M TEAP/CH_3CN.

The question of the site of reduction can be carried one step further by designing complexes where VL is the *first* ligand reduced. In the cyclic voltammograms of the complex $[Ru(HC(pz)_3)(vpy)_3]^{2+}$ (Figure 2A) reduction of the tripyrazolylmethane group is not expected within the potential window of the solvent, based on the electrochemical properties of related complexes. As a consequence, the irreversible wave at $E_{p,c} = -1.56$ V appears to have its origin in the reduction of the vpy ligand (eq 14). Another example of a voltam-

$$[Ru^{II}(HC(pz)_3)(vpy)_3]^{2+} + e^- \rightleftharpoons [Ru^{II}(HC(pz)_3)(vpy^-\cdot)(vpy)_2]^+ \quad (14)$$

metrically observable, direct reduction of a vinyl-containing ligand appears to occur for complexes containing the β-(3-*N*-methylpyridyl)acryloyl group, *N*-Me-py:

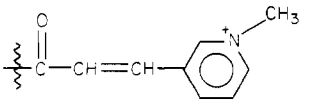

The group was attached to complexes by formation of an amide linkage to a metal-bound pyridyl group. The complex $[Ru(bpy)_2(N\text{-Me-py})_2]^{4+}$, which contains two of the ligands, exhibits a reduction characteristic of the pyridinium group at a potential of −1.0 V vs. SSCE, followed by the expected two reductions at the bipyridine ligands (Table II). Polymer film deposition results at the pyridinium potentials; it occurs more rapidly at the more negative potentials where the bpy ligands are reduced. Another example of the same kind appears for the ferrocene derivative shown in eq 7, where the *only* complex-based reduction occurs at the pyridinium group. Figure 3 shows cyclic voltammograms during polymerization of the ferrocene derivative. With time, the electrode gradually becomes passivated in terms of the wave appearing at the pyridinium potential (irreversible reduction appears to destroy the pyridinium-based redox conductivity of the film) and film growth stops. The ferrocene/ferrocenium couple remains observable in the voltammogram.

Solutions of the complex $[Ru(bpy)_2(4'\text{-OMe-stilb})_2]^{2+}$ show an irreversible oxidative wave at $E_{p,a} = 1.47$ V as well as the usual, reversible Ru(III/II) couple at $E^{\circ\prime}_{soln} = 1.19$ V. These features are also observed for the surface-attached polymeric analogue, but the more positive wave appears only on the *first* potential sweep. The appearance of the second wave is attributable to irreversible oxidation of the methoxy group on the stilbazole ligand.

In addition to electropolymerization, upon reduction the complex $[Ru(bpy)_2(vpy)Cl]^+$ also shows partial substitution of chloride by acetonitrile. The appearance of the nitrile product is evident in voltammograms of both solution and surface film couples.[10b,d] Reductively induced substitution was

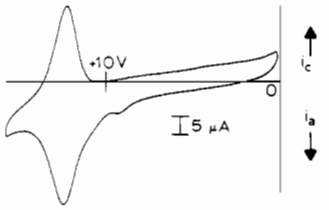

Figure 4. Cyclic voltammogram of $[Ru(bpy)_2(vpy)_2]^{2+}$-based polymer film in fresh electrolyte.

not a problem for the other complexes used in this study.

Structural and Electronic Effects on Film Formation. Determination of Γ/Γ_0. As a first comment on the formation of films by reductive electropolymerization, it should be noted that the procedure adopted here for the initiation of polymerization was based on reductive *cycling* through ligand-based reductions. The advantage of this procedure from the preparative point of view is that it results in uniform, relatively smooth films. Reduction at constant negative potentials also leads to electropolymerization, but the growth rate is faster and the resulting films are clearly less uniform in appearance.

One goal of this study was to probe the sensitivity toward polymerization of vinyl-ligand-containing metal complexes with regard to structure and degree of reduction. The approach we have taken is to measure the apparent polymer film-forming rate for a given complex in a defined state of reduction relative to a standard under otherwise identical conditions. The standard chosen was the complex $[Ru(bpy)_2(vpy)_2]^{2+}$. The procedure followed in making comparisons is as described below. The working-electrode potential was cycled repeatedly through one of the reductive couples of the complex in a solution of known concentration. The resulting, film-coated electrode was transferred to a fresh electrolyte solution, and the apparent surface coverage of electroactive material (Γ_{obsd}) was determined by integration of the charge passed in a 200 mV/s potential sweep through the oxidative component of the metal(III/II) wave in the resulting polymer film. The observed value was normalized by dividing by the concentration of the complex and number of cyclical potential scans used in the electropolymerization. The normalized value was in turn divided by a similarly determined value, Γ_0, for the complex $[Ru(bpy)_2(vpy)_2]^{2+}$ obtained by cycling through the first reduction couple of this complex. The resulting ratio, Γ/Γ_0, provides a semiquantitative measure of the intrinsic polymerizability of any complex relative to that of the reference complex. An example of the procedure is described below.

Polymerization of a 0.1 M $TEAP/CH_3CN$ solution of $[Ru(bpy)_2(vpy)_2]^{2+}$ (1.64 mM) by cycling the electrode potential 145 times between −0.9 and −1.5 V (the first reduction of the complex occurs at −1.36 V) gave an electrode whose dried surface was gold in color and which gave the (typical) oxidative voltammogram in Figure 4. The surface wave is nearly Nernstian by its stable, symmetrical shape with $E^{\circ\prime}$ = 1.22 V, ΔE_p = 25 mV, and E_{fwhm}[33] = 170 mV.[37] Also present is a small anodic prewave, a common feature in voltammetry of these electrochemically produced films whose chemical origin is not understood and will not be discussed further. Γ_{obsd} for the experiment was found to be 1.57×10^{-9} mol/cm^2, which is normalized by[38]

$$\Gamma_0 = \Gamma_{obsd}/(\text{no. of scans})[\text{complex}] = 6.6 \times 10^{-9}$$

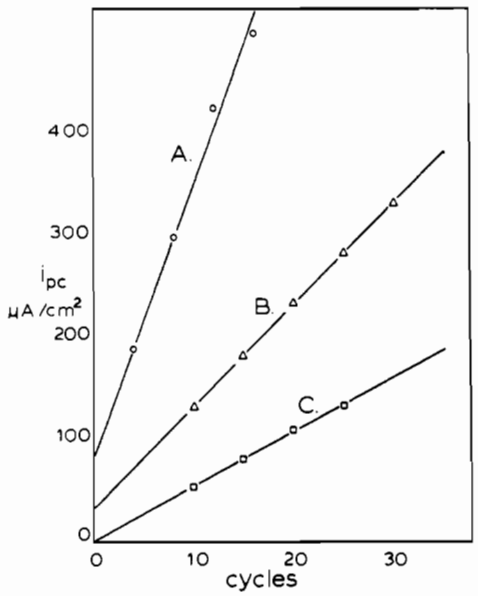

Figure 5. Cathodic current for the first bpy reduction of $[Ru(bpy)_2(p\text{-cinn})_2]^{2+}$ vs. the number of reductive cycles at various [complex]: (A) 0.71 mM; (B) 0.33 mM; (C) 0.18 mM. The nonzero intercepts are apparently a consequence of rapid initial polymerization on the first few cycles.

In another experiment, a polymer film of the same complex was formed on a freshly polished electrode, but the negative potential limit was extended to −1.7 V, to include the second bpy-based reduction at −1.54 V. The number of potential cycles was 118. Γ_{obsd} for this polymer film was 4.8×10^{-9} mol/cm^2. The calculation for Γ/Γ_0 is then

$$\Gamma = 4.77 \times 10^{-9}/(118)(1.64 \times 10^{-3}) = 2.5 \times 10^{-8}$$

$$\Gamma/\Gamma_0 = 2.5 \times 10^{-8}/6.6 \times 10^{-9} = 3.7$$

The resulting value of Γ/Γ_0 indicates that the doubly reduced complex $[Ru(bpy)_2(vpy)_2]^0$ yields 3.7 times more electroactive, polymeric material on the electrode surface than the singly reduced complex under equivalent conditions. Values for Γ/Γ_0 determined by using the same approach are listed in Table II for all of the new polymerizable monomers. The relative polymerization coverages resulting from cycling through the first or second reductions of a complex are designed $(\Gamma/\Gamma_0)_1$ and $(\Gamma/\Gamma_0)_2$, respectively.

There are several caveats in the Γ/Γ_0 data that are important in comparing the behavior of various complexes. First, unless the film is very stable, the measured coverage Γ_{obsd} is less than that originally deposited on the surface and Γ/Γ_0 does not accurately reflect the inherent polymerizability of the complex. The stability of these films, however, appears to be quite good, especially for oxidative cycling. Second, the rate of charge transport through the film must be fast relative to the time scale of the potential sweep so as to ensure the response of redox sites throughout the entire film. When Γ_{obsd} is $<10^{-8}$ mol/cm^2, the value of Γ_{obsd} determined at 200 mV/s is the same as that at slower sweep rates. Third, a tacit assumption in the normalization of Γ_{obsd} with respect to concentration and number of potential scans is that the quantity of electroactive polymer is proportional to concentration and the number of reductive cycles. This is in fact true[39] for

(37) For theoretical descriptions of the expected voltammetric wave shapes for reactants (polymeric and otherwise) confined to an electrode surface, see: (a) Brown, A. P.; Anson, F. C. *Anal. Chem.* **1977**, *49*, 1589–95. (b) Laviron, E. *J. Electroanal. Chem. Interfacial Electrochem.* **1979**, *100*, 263–70. (c) Laviron, E. *Ibid.* **1980**, *112*, 1–9. (d) Laviron, E.; Roullier, L.; Degrand, C. *Ibid.* **1980**, *112*, 11–23. (e) Laviron, E. *Ibid.* **1981**, *122*, 37–44. (f) Smith, D. F.; Willman, K.; Kuo, K.; Murray, R. W. *Ibid.* **1979**, *95*, 217–27. (g) Reference 2b.

(38) The units of this parameter (L/cm^2) are not those of surface coverage (mol/cm^2). However, since the actual value of Γ is not crucial, the nomenclature is used for convenience. Γ values should also not be interpreted as reflecting the thickness of the film since the concentration term used here is for the complex in solution, not for sites within the film.

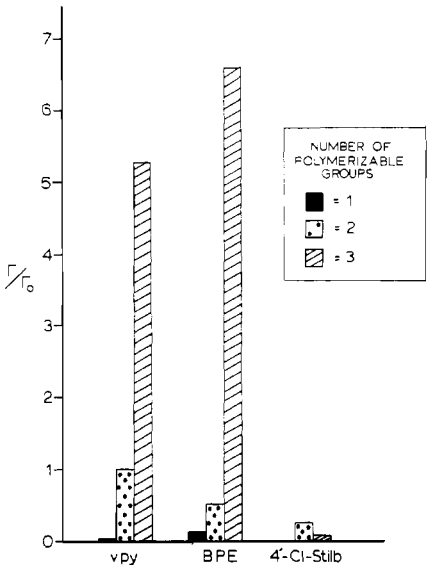

Figure 6. Relationship between normalized surface coverage and the number of polymerizable groups in the complexes $[Ru(trpy)(bpy)(L)]^{2+}$, $[Ru(bpy)_2(L)_2]^{2+}$, and $[Ru(trpy)(L)_3]^{2+}$ (L = vpy, BPE, 4'-Cl-stilb).

$[Ru(bpy)_2(vpy)_2]^{2+}$ but only for certain combinations of concentration and number of cycles. For a given concentration Γ_{obsd} increases linearly with the number of scans only up to a certain point, after which further cycling yields proportionately smaller increases in the deposition of material on the electrode. Fewer scans are necessary to reach the limiting coverage at higher concentrations and vice versa. At low monomer concentrations ($\leq$2 mM) the deposition rate is typically constant up to at least 30 cycles and is directly proportional to the monomer concentration, as shown in Figure 5 by the cathodic current for the first bpy reduction as a function of the number of scans for three concentrations of the complex $[Ru(bpy)_2(p\text{-cinn})_2]^{2+}$. Clearly, values of Γ/Γ_0 have meaning only when the conditions of the experiment correspond to the linear region of the polymer growth curve. Unfortunately, generation of such curves for each of the 2, complexes investigated here would have been too time consuming. However, in our experiments we have repeated the polymerization experiment for each complex several times, using differing numbers of potential scans and, in some cases, also using different concentrations of complex. Clearly nonlinear growth curves seem to be most often encountered for complexes of the type $M(chel)(VL)_3^{2+}$ as reflected in the wide range of Γ/Γ_0 values reported for these materials.

Despite these drawbacks, Γ/Γ_0 is a useful parameter. For example, in the construction of multiply layered surfaces, it is important to be able to produce layers of predetermined thicknesses. Thickness is also important to film permeability. If Γ/Γ_0 is known for the monomer, the proper combination of complex concentration and number of potential scans required to prepare the desired layer thickness can easily be calculated.

As shown below, the Γ/Γ_0 values give insight into those factors that control the electropolymerization process, including (i) the number of polymerizable ligands in the complex, (ii) direct vs. indirect reduction of the vinyl-containing ligand and the dependence on negative electrode potential limit, (iii) steric hindrance at the vinyl group, and (iv) reductive adsorption of the monomer complexes.

Effect of the Number of Polymerizable Groups. One of the most apparent trends in the Γ/Γ_0 data is the greater polymerizability of monomers as the number of coordinated vinyl ligands increases. This is illustrated in Figure 6 with $(\Gamma/\Gamma_0)_1$ values for films produced by cycling through the first reductions for the series of complexes $[Ru(trpy)(bpy)(L)]^{2+}$, $[Ru(bpy)_2(L)_2]^{2+}$, and $[Ru(trpy)(L)_3]^{2+}$ (L = vpy, BPE, and 4'-Cl-stilb). When L = vpy, the reductive polymerizability for the series of monomers tris:bis:mono is 250:50:1. The trend is equally pronounced when the potential sweep is extended to include the second reduction, $(\Gamma/\Gamma_0)_2$, where for the vpy series the ratios are 1260:42:1, respectively.

One explanation for the dependence of the number of polymerizable groups is that metallopolymers containing three polymerizable groups per monomeric unit are likely to be highly cross-linked and hence less soluble than polymers having only two or one polymerizable group. As a consequence, even relatively short-chain, oligomeric materials could have limited solubilities and begin to deposit on the electrode rather than diffuse away into the solution. Another possible reason is that monomers with multiple sites for polymerization have a greater probability of attaining a favorable orientation with respect to incorporation into the growing polymer network. A third consideration is that increasing the number of groups statistically favors formation of the radical anion initiator in the intramolecular redox equilibrium expression. This will be further examined in the next section.

Complexes of the stilbazoles are anomalous in that they generally yield substantially lower surface coverages than the vpy or BPE analogues, regardless of the number of stilbazole ligands present. This is possibly due to greater solubility of the stilbazole monomer with consequent slower deposition of the resulting polymeric metal complex chains.

Dependence of Γ/Γ_0 on the Extent of Reduction and Direct vs. Indirect Reduction of the Vinyl Ligand. A second trend readily discernible in Table II is the effect of sweeping the electrode potential through the first or second ligand-based reduction waves for the complex. Substantially greater coverage typically results from cycling through the second reduction wave. This is particularly evident for complexes of the type $[Ru(trpy)(VL)_3]^{2+}$. To understand this dependence of Γ/Γ_0, a few words need to be said about the basic concept of the polymerization reaction.

The idea for reductive electrochemical polymerization of transition-metal complexes[10d] was based on the knowledge that reductions of Ru(II) poly(pyridyl) complexes are ligand localized in character (see eq 8–13) and that 4-vinylpyridine is amenable to anionically initiated polymerization.[40] It was reasoned that reduction of a complex like $[Ru(bpy)_2(vpy)_2]^{2+}$ would generate, through ligand orbital mixing, radical anion character at the vpy ligand or, at least, an electronic pathway for ligand to ligand electron hopping. It was hoped that the net effect would be the induced polymerization (and deposition onto the electrode) of the complex. The hypothesis was borne out experimentally, indicating that reduction does lead to vpy radical anion character. It is important to note that polymerization occurs for $[Ru(bpy)_2(vpy)_2]^{2+}$ even though the initial reductive process occurs at a largely π^*(bpy) level (eq 8, 9). A convenient term to describe the polymerization process in such cases is that the polymerization is indirect in that the initial site of reduction is *not* at the polymerizable ligand.

On the other hand, for certain complexes the polymerizable ligand is the site of initial reduction at the electrode (cf. eq 13, 14) and it is convenient to describe the polymerization process as being *direct* in such cases.

The example shown in eq 14 involves a complex that was synthesized specifically to explore the efect of direct reduction of coordinated vinylpyridine. As evidenced by the large value

(39) Ellis, C. D.; Murphy, W. R.; Meyer, T. J., unpublished results.

(40) Kalir, R.; Zilkha, E. *Eur. Polym. J.* **1978**, *14*, 557–62.

of Γ/Γ_0 for the complex, direct reduction at the vpy ligand apparently leads to rapid polymerization and extensive deposition of the resulting tripyrazolylmethane-containing polymer. A related situation is encountered for the complexes $Ru(trpy)(L)_3^{2+}$ (L = vpy, BPE) in the *second* reduction wave (eq 13), which appears to be a direct, VL-localized process. $(\Gamma/\Gamma_0)_2$ values for the (vpy), and BPE complexes are 31 and 25 times greater than those obtained by cycling through only the first, trpy-localized reduction. The experiment provides a graphic example of how the choice of the negative potential limit on a reductive scan can determine the apparent rate of polymerization and, in this case, the value of direct reduction at the polymerizable ligand.

Due to potential range limitations, direct initiation is possible with relatively few of the complexes reported here. Most of the monomers were polymerized via the indirect process, with initial reduction occurring at a bpy and/or a trpy ligand. Polymerization could be induced following one-electron reduction based on the intramolecular redox equilibrium shown in eq 15 between the oxidation-state isomers involving the

$$[Ru^{II}(bpy)(bpy^{-}\cdot)(VL)_2]^+ \underset{\Delta E°(red)}{\overset{K'}{\rightleftharpoons}} [Ru^{II}(bpy)(bpy^0)(VL)(VL^{-}\cdot)]^+ \quad (15)$$

poly(pyridyl) radical anion and the thermodynamically less favored isomer in which the added electron is localized on the VL ligand. The K' value for eq 15 cannot be calculated because an $E_{1/2}$ value is not available for the high-energy, ligand-based oxidation-state isomer. However, for the complex $Ru(trpy)(vpy)_3^{2+}$ $E°'$ values are available for the couples $Ru(trpy)(vpy)_3^{2+}/Ru(trpy)(vpy)_3^{+}$ (−1.24 V) and $Ru(trpy)(vpy)_3^{+}/Ru(trpy)(vpy)(vpy)_2^{0}$ (−1.76 V). From the data an equilibrium constant can be calculated for the comproportionation reaction in eq 16a, which represents an alternate

$$Ru^{II}(trpy^{-}\cdot)(vpy)_3^{+} \rightarrow {}^1/_2Ru(trpy)(vpy)_3^{2+} + {}^1/_2Ru^{II}(trpy^{-}\cdot)(vpy^{-}\cdot)(vpy)_2^{0} \quad (16a)$$

route for obtaining VL-based reduced complexes, $K = 10^{16.9n(\Delta E°'(red))} = 3 \times 10^{-9}$. As noted above, an $E°'$ value cannot be measured for the vpy-based couple in a complex containing unreduced trpy or bpy, e.g., $Ru(trpy)(vpy)_3^{2+}/Ru(trpy)(vpy^{-}\cdot)(vpy)_2^{+}$. However, it seems obvious that $\Delta E°'(redox) = -0.52$ V for eq 16a represents an upper limit for the vpy-based couple and for the intramolecular redox equilibrium in eq 16b, $K > 10^{-9}$. In any case, it is certainly

$$Ru(trpy^{-}\cdot)(vpy)_3^{+} \rightarrow Ru(trpy)(vpy^{-}\cdot)(vpy)_2^{+} \quad (16b)$$

expected that the extent of polymerization as viewed through Γ/Γ_0 values should be dependent upon $\Delta E°'(red)$.

From Table II it can be seen that the first bipyridine reduction, $E°'(red,1)_{soln}$, for the series of complexes $[Ru(bpy)_2(4'\text{-X-stilb})_2]^{2+}$ (X = OMe, H, Cl, CN) is essentially constant at −1.38 ± 0.02 V. However, the electron-withdrawing or -donating character of X should exert a strong influence on the reduction potential of the stilbazole ligand, and therefore on $\Delta E°'(redox)$. In Figure 7 is shown a plot of log $(\Gamma/\Gamma_0)_1$ for these complexes as a function of the Taft–Hammett[41] parameter for the different X substituents. It is expected that $E°'$ for the VL-based reduction will also parallel σ_p on the basis of substituent effects, so that the increase in log $(\Gamma/\Gamma_0)_1$ is presumably paralleled by a *decrease* in $\Delta E°'(redox)$. The linear plot supports the contention that, in an indirect initiation process, a determining factor in the rate of polymerization, and consequently the rate of film formation, is the concentration of the reactive radical anion as controlled by $E°'(redox)$ and K.

(41) Lowry, T. H.; Richardson, K. S. "Mechanism and Theory in Organic Chemistry"; Harper and Row: New York, 1976; p 62.

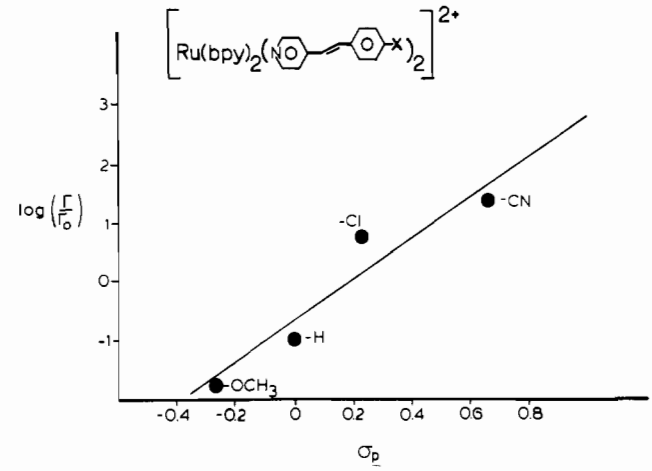

Figure 7. Linear relation between the Taft–Hammet σ_p and the logarithm of normalized surface coverage for the complexes $[Ru(bpy)_2(L)_2]^{2+}$ (L = 4′-substituted-4-stilbazole).

Table III. Film-Formation Efficiencies[a] for Selected Complexes

complex	$\Phi(poly)_1$[b]	$\Phi(poly)_2$[c]
$[Ru(bpy)_2(vpy)_2]^{2+}$	0.003	0.011
$[Ru(trpy)(vpy)_3]^{2+}$	0.020	0.34[d]
$[Ru(bpy)_2(p\text{-cinn})_2]^{2+}$		0.07–0.12
$[Os(bpy)_2(vpy)_2]^{2+}$	0.0078	0.084
$[Ru(trpy)(bpy)(vpy)]^{2+}$	6×10^{-5}	3.9×10^{-4}
$[Ru(HC(pz)_3)(vpy)_3]^{2+}$	0.50[d]	
$[Ru(bpy)_2(vpy)Cl]^{+}$	5×10^{-5}	
$[Ru(trpy)(4'\text{-Cl-stilb})_3]^{2+}$	2.1×10^{-4}	1.03[d]
$[Ru(phen)_2(vpy)_2]^{2+}$	0.0013	0.065

[a] Efficiencies are defined as mol of polymer deposited on electrode/(mol of monomer complex reduced/cycle). [b] Potential was cycled through only the first reduction of the complex. [c] Potential was cycled through first and second reductions. [d] Direct reduction of vinyl ligand (direct initiation process).

Steric and Adsorption Effects on Surface Coverages. The data in Table II reveal, somewhat surprisingly, no particular inhibition of film formation when the vinyl-containing ligand has greater steric bulk. For example, the surface coverages of $[Ru(bpy)_2(vpy)_2]^{2+}$ and $[Ru(bpy)_2(BPE)_2]^{2+}$ are similar even though the additional pyridine group at the polymerizable site might be expected to create steric problems.

Another interesting comparison is between $[Ru(phen)_2(vpy)_2]^{2+}$ and $[Ru(bpy)_2(vpy)_2]^{2+}$. The parameter $(\Gamma/\Gamma_0)_2$ is 4 times higher for the phen complex compared to that for the bpy complex for reduction of the second ligand (see Table II). A major difference in the solution electrochemistry of the analogous pyridyl derivatives lies in the observation that for the phen complex, $[Ru(phen)(py)_2]^{2+}$, the reverse oxidation wave following the second phen reduction is large and the wave shape noticeably sharpened, indicating adsorption of the doubly reduced species. The wave shape for the bpy complex is normal.[42] This observation suggests that adsorption at the electrode can play a role in leading to enhanced polymer surface coverages.

Mechanism of Reductive Electrochemical Polymerization. As discussed in a previous section, the indirect initiation process is thought to involve transfer of an electron to a VL ligand by intramolecular electron transfer (eq 15) or comproportionation (eq 16). In either case, from $\Delta E°'(redox)$ values

(42) The electrochemistry of the bpy complex has been reported in: Salmon, D. J. Ph.D. Dissertation, The University of North Carolina, Chapel Hill, NC, 1976. Data for the phen complex is from: Salmon, D. J., unpublished results. Cyclic voltammetry of the complex $Ru(phen)_3^{2+}$ has been described in: (a) Kahl, J. K.; Hanck, K. W.; DeArmond, K. *J. Phys. Chem.* **1979**, *83*, 2611–5. (b) Tokel-Takvoryan, N. E.; Hemingway, R. E.; Bard, A. J. *J. Am. Chem. Soc.* **1973**, *95*, 6582–9.

Scheme I

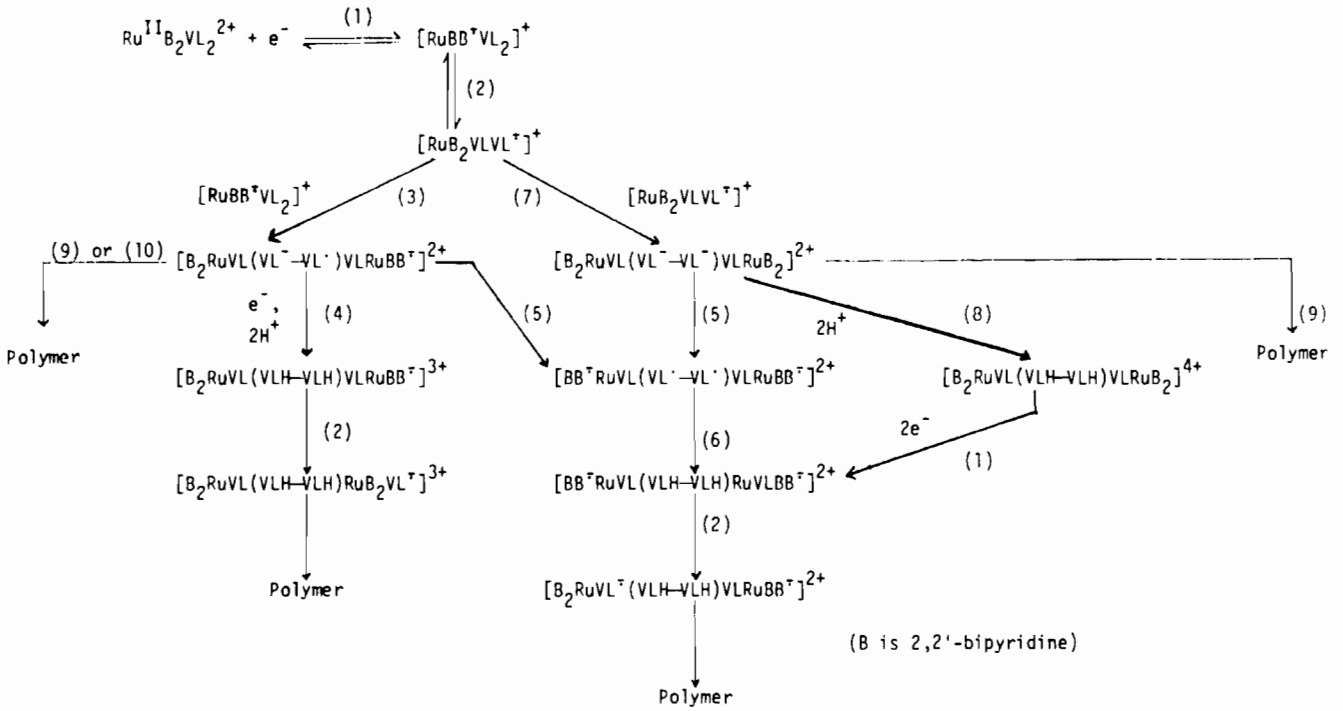

estimated from differences in reduction potentials between the poly(pyridyl) and vinyl ligands (see Table II), it is predicted that very small populations of the reduced vinyl ligand form exist, and hence low efficiencies (Φ_{poly}) for the polymerization and film-forming processes might be expected. However, experimentally determined current efficiencies (see Table III) can be quite substantial, ranging from 0.006% for $[Ru(trpy)(bpy)(vpy)]^{2+}$ to 2.0% for $[Ru(trpy)(vpy)_3]^{2+}$ for experiments involving only the first monomer reduction wave. Direction initiation gives even higher values for Φ_{poly} and reflects the effect of bypassing eq 15. For most complexes in Table III the polymerization reaction appears to be much more efficient than would be expected on the basis of an intramolecular redox equilibrium like eq 15. Thus the overall mechanism for the polymer growth process must deal with this apparent contradiction.

A number of mechanistic pathways can be conceived of for the polymer chain growth process. Representing a typical monomer with two bpy (B) and two vinylic ligands (VL), as $[Ru(B)_2(VL)_2]^{2+}$, Scheme I depicts various reaction pathways following one-electron reduction (eq 8) and intramolecular electron transfer (eq 15) in the monomer complex.

In Scheme I, the reactive radical anion (generated by either direct or indirect initiation) may either (i) undergo radical–radical dimerization, step 7, or (ii) react with a bpy-reduced monomer (radical–substrate coupling), step 3. The dimers formed in steps 3 and 7 can yield hydro dimers by a variety of paths. The dimers formed in either case may protonate (steps 4, 8) to yield hydrogenated dimer. In either case, if the initiation step involves indirect reduction at VL by intramolecular electron transfer, the VL-based anion can undergo a reverse, intramolecular electron transfer (step 5) to generate a radical site and regenerate a reduced bpy ligand site, e.g.

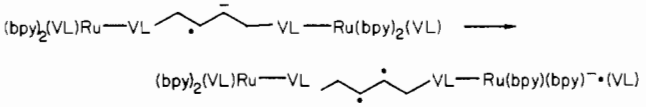

The diradical so formed could collapse to an (isolated) olefin site or abstract hydrogen atoms from the acetonitrile solvent to yield hydrogenated dimer (step 6). In step 5 it is important to note that the electron used to reduce the complex (step 1) and generate the reactive radical (step 2) has been recycled to the bpy ligand and so is available for intramolecular transfer to the second VL ligand site. Thus, the sequence of steps 2, 7, 5, 6 can be repeated.

The dimers formed in steps 3 and 7 may also participate in classical polymerization processes, that formed in step 7 initiating anionic polymerization with chain growth at both sites of the dimer and that formed in step 3 initiating radical-based polymerization. Since complexes having a single vinyl ligand undergo film deposition[10a,b,d,12c,f] albeit with relatively low Γ/Γ_0 values, radical and/or anionic chain growth pathways must also exist since only soluble, dimeric complexes would result from hydrodimerization. Even sterically hindred vinyl complexes like the ferrocene derivative (eq 7) undergo deposition by what must be a classical polymerization process. Monomers with a single polymerizable group generally form films 20–50 times less rapidly than similar complexes having two vinyl-containing ligands (see Γ/Γ_0 values, Table II). Polymerization efficiencies for monovinyl complexes are also much lower (Table III). The differences between complexes having single and multiple vinyl groups are more than statistical and clearly suggest that chain propagation occurring via a sequence of successive hydrodimerizations (e.g., steps 7, 5, 6) may be at least as important as the radical or anionic polymerization routes.

Copolymerization experiments with structurally similar monomers were used to evaluate the relative contributions of the two types of pathways. The vinyl-containing amide complexes are particularly convenient for such studies because of the simplicity of synthetic variation of monomers; however, it is probable that other ligand systems such as vpy or BPE exhibit similar behaviors.

Electroreductive polymerization of solution mixtures of $[Ru(bpy)_2(p\text{-cinn})_2]^{2+}$ and $[Os(bpy)_2(p\text{-cinn})_2]^{2+}$ deposits films containing both complexes. The relative charges under the well-resolved $M^{3+/2+}$ oxidative voltammetric waves are the same as the relative concentration of monomers in the deposition solution. The monomers seem equally reactive, consistent with their nearly equal (Γ/Γ_0) values in Table II. Variable-angle XPS of the characteristic Ru and Os binding energies on the electrode surface confirm this and also dem-

Table IV. Mole Fraction of Ru Complex Present in $Ru(bpy)_2(m\text{-cinn})_2^{2+}/Os(bpy)_2(p\text{-cinn})_2^{2+}$ Mixtures

x_{soln}[a]	x_{surf}[b]	x_{surf}/x_{soln}	x_{soln}[a]	x_{surf}[b]	x_{surf}/x_{soln}
0.33	0.26	0.79	0.68	0.50	0.74
0.52	0.37	0.71			

[a] Fraction of Ru present in deposition solutions. [b] Fraction of Ru present in surface-bound polymer film after polymerization of monomer solution mixture.

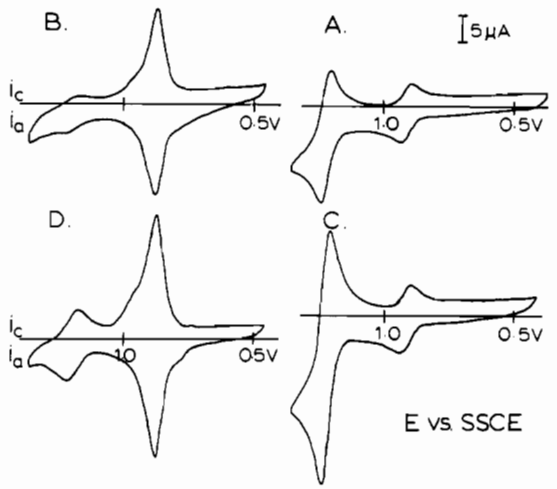

Figure 8. Cyclic voltammograms of mixtures of $[Ru(bpy)_2(p\text{-}CH_2\text{-cinn})_2]^{2+}$ and $[Os(bpy)_2(p\text{-cinn})_2]^{2+}$ ($\sim 5 \times 10^{-4}$ M): (A, C) deposition solution mixtures; (B, D) copolymer films in fresh electrolyte after electropolymerization of solutions in A and C, respectively.

onstrate that a homogeneous copolymer has been formed.[43] Polymerization of a different mixture, $[Os(bpy)_2(p\text{-cinn})_2]^{2+}$ and $[Ru(bpy)_2(m\text{-cinn})_2]^{2+}$, results in copolymers with a smaller fraction of ruthenium in the film than in the solution mixture (Table IV), and (Γ/Γ_0) in Table II shows that deposition of the ruthenium *m*-cinn complex is about 3 times slower than that of the osmium monomer. These results demonstrate that both concentrations and relative polymerization rates are important in determining copolymer compositions formed from solutions containing two electropolymerizable monomers.

A third copolymer experiment was carried out for the mixture $[Os(bpy)_2(p\text{-cinn})_2]^{2+}$ and $[Ru(bpy)_2(p\text{-}CH_2\text{-cinn})_2]^{2+}$. This is an interesting experiment since the latter monomer does not undergo electropolymerization alone ($\Gamma/\Gamma_0 = 0$). Figure 8 shows the $M^{3+/2+}$ voltammetry of the monomer mixture and of the copolymer film. Some ruthenium complex is clearly deposited, but even when the ruthenium complex monomer concentration is in large excess over the osmium comonomer, only a small amount of Ru is incorporated into the polymer film. This result strongly suggests that for monomers having more than one polymerizable ligand the classical anionic and/or radical chain growth pathways contribute relatively little to overall film formation and that the more efficient hydrodimerization pathways are mainly responsible for chain propagation.

Further evidence for predominance of the hydrodimerization pathways comes from copolymers formed by reducing mixtures of $[Ru(i\text{-Pr-bpy})_2(p\text{-cinn})_2]^{2+}$ with $[Ru(bpy)_2(p\text{-cinn})]^{2+}$ or $[Ru(bpy)_2(vpy)_2]^{2+}$. The bpy-ester complex is reduced electrochemically at potentials much more positive than the unsubstituted bpy reductions in the other two complexes and does not form polymer by itself. Cyclic voltammograms of solution

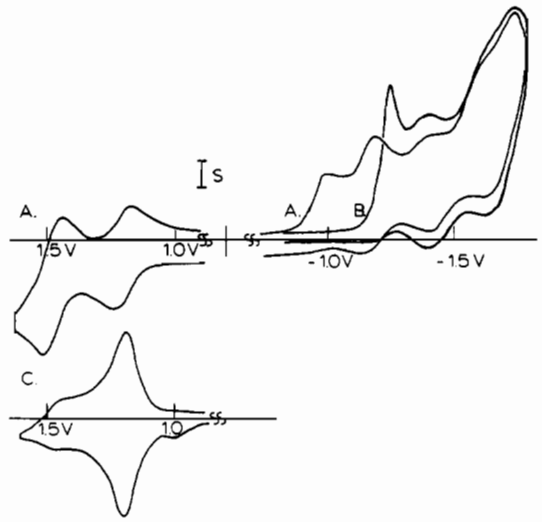

Figure 9. Cyclic voltammograms of a mixture of $[Ru(bpy)_2(p\text{-cinn})_2]^{2+}$ and $[Ru(i\text{-Pr-bpy})_2(p\text{-cinn})_2]^{2+}$ ($\sim 5 \times 10^{-4}$ M) in solution and as a copolymer film ($S = 10$ μA): (A) complexes in solution; (B) mixture after 10 reductive cycles; (C) copolymer films in clean electrolyte after B.

oxidation of a mixture of the two cinnamide monomers (curve D), reductive deposition (curves A and B) and the oxidation of the resultant polymer film in fresh electrolyte (curve C) are shown in Figure 9. The two monomer solution concentrations are approximately equal. The first reductive cycle (curve A) shows reduction waves for first the ester-bpy and then the bpy complex. After 10 reductive cycles (curve B) the ester-bpy reduction now occurs as a mediated reduction through the deposited $[Ru(bpy)_2(p\text{-cinn})_2]^{2+}$ film. The oxidative voltammogram of the film surface (curve C) shows incorporation of only small amounts of $[Ru(i\text{-Pr-bpy})_2(p\text{-cinn})_2]^{2+}$. In this case, only the complex that can transfer significant radical anion character to the cinnamamide ligand undergoes polymerization, even though both complexes bear identical cinnamamide groups. This is another example of the importance of $\Delta E^{\circ\prime}$(redox) on the rate of polymerization: $E^{\circ\prime}$(red,1) is shifted positively by 430 mV for the ester-bpy complex, compared to that for the unsubstituted bpy analogue. Thus, not only do the classical polymer chain growth processes (step 9) appear to be much slower than hydrodimerization but also attack of a monomer radical anion on an unreactive, reduced monomer (e.g., step 3 with $[Ru(bpy)(bpy^{-}\cdot)(VL)_2]^{+}$) seems to contribute little to the polymerization process. The observation that copolymerization of $[Ru(bpy)_2(vpy)_2]^{2+}$ with $[Ru(i\text{-Pr-bpy})_2(p\text{-cinn})_2]^{2+}$ also yields little incorporation of the ester/cinnamamide complex indicates that even a complex with unhindered vinyl groups mainly undergoes reductive dimerization.

From the above experiments, the most likely pathway to oligomerization of the monomers containing cinnamamide ligands appears to be a reactive radical–reactive radical coupling mechanism (step 7) followed by steps 5, 6 or 8, 1 to yield hydro dimers. This is promoted by the high local concentrations of radical anions at the electrode surface. Szwarc has noted that for 1,1-diphenylethylene the radical anion dimerization rate is 1000 times faster than attack of a radical anion on an unreduced monomer.[44] Electroreductive hydrodimerization via radical–radical coupling has also been observed for several activated olefins.[45] Coupling of ethyl cin-

(43) Facci, J. S.; Schmehl, R. H.; Murray, R. W. *J. Am. Chem. Soc.* **1982**, *104*, 4959.

(44) Swarc, M. "Carbanions, Living Polymers and Electron Transfer Processes"; Interscience: New York, 1968; pp 367–78.

(45) (a) Puglisi, V. J.; Bard, A. J. *J. Electrochem. Soc.* **1972**, *119*, 829–33. (b) Bard, A. J.; Puglisi, V. J.; Kenkel, J. V.; Lomas, A. *Discuss. Faraday Soc.* **1973**, 353–66.

namate, a molecule quite similar to the active portion of the above complexes, yields hydro dimers via what is believed to be a radical–radical coupling process.[45] Finally, we should emphasize that the hydro dimer formed from $[Ru(bpy)_2(p\text{-}cinn)_2]^{2+}$ has two unreacted cinnamamide groups remaining which can participate in further coupling reactions, resulting in chain growth.

The relatively high efficiencies observed for polymer formation despite the unfavorable intramolecular electron-transfer step 2 may be explained by the reverse intramolecular electron-transfer pathway in step 5. The resulting alkyl radical intermediates may form olefin or the hydro dimer product via atom abstraction from solvent (step 6), and the reduced bpy may once again undergo intramolecular redox reaction with a vinyl-containing ligand to form a reactive radical which can undergo further reaction via steps 7, 5, and 6. Thus the hydro dimer formed in steps 5 and 6 need not be rereduced at the electrode surface in order to undergo further coupling, and it can be oxidized by the electrode or by self-exchange in solution without destruction of an essential polymer-propagating site. This may explain why the film-forming process proceeds effectively even though the potential cycling experiment alternately starts and stops the polymerization reaction. Finally, we should note that, in the repetitive step 2, 7, 5, 6 pathway, the polymer chain incorporates the metal complex as a structural element, as opposed to a pendant group, and cross-linking of chains is likely.

From the results presented, it is evident that both polymer chain growth and hydrodimerization are involved in polymerization reactions that eventually deposit films on electrode surfaces. The chemical and electrochemical differences between the films formed by each mechanism are subtle and we have as yet no evidence to suggest that films formed by different means have distinguishable sites. Undoubtedly, the relative rates of polymerization and hydrodimerization are controlled principally by relative reactivity of the vinyl anion radicals formed, although the steric environment may also contribute to a lesser degree. For the above complexes with anion radicals stabilized by extensive conjugation and having considerable steric crowding, the hydrodimerization mode of polymerization is clearly preferred. Such a pathway limits the variety of copolymers that can be prepared by this type of surface derivatization, since all species participating in the copolymerization must be able to couple upon reduction. However, the electropolymerization chemistry does provide a simple method for obtaining a wide variety of uniform, electrochemically active films of predetermined thickness and widely varying permeability.[12a]

Acknowledgment. This research was supported by grants to T.J.M. and R.W.M. from the National Science Foundation. XPS experiments were performed by D. Griffis in the UNC Surface Analysis Facility.

(46) Klemm, L. H.; Olson, D. R. *J. Org. Chem.* **1973**, *38*, 3390–4.

Registry No. $[Ru(trpy)(bpy)(vpy)](ClO_4)_2$, 85661-58-1; $[Ru(trpy)(bpy)(vpy)](ClO_4)_2$ (polymer), 85661-69-4; $[Ru(trpy)(bpy)(vpy)]^{3+}$, 85649-75-8; $[Ru(trpy)(bpy)(BPE)](PF_6)_2$, 85661-59-2; $[Ru(trpy)(bpy)(BPE)](PF_6)_2$ (polymer), 85649-77-0; $[Ru(trpy)(bpy)(BPE)]^{3+}$, 85661-70-7; $[Ru(trpy)(bpy)(4'\text{-Cl-stilb})](PF_6)_2$, 85717-51-7; $[Ru(trpy)(bpy)(4'\text{-Cl-stilb})](PF_6)_2$ (polymer), 85649-78-1; $[Ru(trpy)(bpy)(4'\text{-Cl-stilb})]^{3+}$, 85661-95-6; $[Ru(bpy)_2(vpy)Cl]PF_6$, 79813-97-1; $[Ru(bpy)_2(vpy)Cl]^{2+}$, 85661-96-7; $[Os(bpy)_2(vpy)Cl]PF_6$, 85661-65-0; $[Os(bpy)_2(vpy)Cl]^{2+}$, 85661-71-8; $[Os(bpy)_2(BPE)Cl]PF_6$, 85661-67-2; $[Os(bpy)_2(BPE)Cl]^{2+}$, 85661-72-9; $[Ru(bpy)_2(vpy)_2](PF_6)_2$, 79813-96-0; $[Ru(bpy)_2(vpy)_2](PF_6)_2$ (polymer), 85649-79-2; $[Ru(bpy)_2(vpy)_2]^{3+}$, 85661-74-1; $[Os(bpy)_2(vpy)_2](PF_6)_2$, 85661-63-8; $[Os(bpy)_2(vpy)_2](PF_6)_2$ (polymer), 85649-81-6; $[Os(bpy)_2(vpy)_2]^{3+}$, 85661-75-2; $[Ru(bpy)_2(BPE)_2](PF_6)_2$, 58167-47-8; $[Ru(bpy)_2(BPE)_2](PF_6)_2$ (polymer), 85700-64-7; $[Ru(bpy)_2(BPE)_2]^{3+}$, 85661-76-3; $[Ru(bpy)_2(stilb)_2](PF_6)_2$, 85717-43-7; $[Ru(bpy)_2(stilb)_2](PF_6)_2$ (polymer), 85700-65-8; $[Ru(bpy)_2(stilb)_2]^{3+}$, 85661-77-4; $[Ru(bpy)_2(4'\text{-Cl-stilb})_2](PF_6)_2$, 85717-45-9; $[Ru(bpy)_2(4'\text{-Cl-stilb})_2](PF_6)_2$ (polymer), 85700-67-0; $[Ru(bpy)_2(4'\text{-Cl-stilb})_2]^{3+}$, 85661-78-5; $[Ru(bpy)_2(4'\text{-OMe-stilb})_2](PF_6)_2$, 85717-48-2; $[Ru(bpy)_2(4'\text{-OMe-stilb})_2](PF_6)_2$ (polymer), 85700-69-2; $[Ru(bpy)_2(4'\text{-OMe-stilb})_2]^{3+}$, 85661-79-6; $[Ru(bpy)_2(4'\text{-CN-stilb})_2](PF_6)_2$, 85717-47-1; $[Ru(bpy)_2(4'\text{-CN-stilb})_2](PF_6)_2$ (polymer), 85760-64-1; $[Ru(bpy)_2(4'\text{-CN-stilb})_2]^{3+}$, 85661-80-9; $[Ru(bpy)_2(p\text{-cinn})_2](PF_6)_2$, 85700-62-5; $[Ru(bpy)_2(p\text{-cinn})_2](PF_6)_2$ (polymer), 85717-39-1; $[Ru(bpy)_2(p\text{-cinn})_2]^{3+}$, 85661-81-0; $[Os(bpy)_2(p\text{-cinn})_2](PF_6)_2$, 85717-52-8; $[Os(bpy)_2(p\text{-cinn})_2](PF_6)_2$ (polymer), 85717-41-5; $[Os(bpy)_2(p\text{-cinn})_2]^{3+}$, 85661-82-1; $[Ru(bpy)_2(m\text{-cinn})_2](PF_6)_2$, 85661-50-3; $[Ru(bpy)_2(m\text{-cinn})_2](PF_6)_2$ (polymer), 85661-40-1; $[Ru(bpy)_2(m\text{-cinn})_2]^{3+}$, 85661-83-2; $[Ru(bpy)_2(p\text{-}CH_2\text{-cinn})_2](PF_6)_2$, 85661-52-5; $[Ru(bpy)_2(p\text{-}CH_2\text{-cinn})_2]^{3+}$, 85661-84-3; $[Ru(bpy)_2(p\text{-fum})_2](PF_6)_2$, 85661-53-6; $[Ru(bpy)_2(p\text{-fum})_2](PF_6)_2$ (polymer), 85661-42-3; $[Ru(bpy)_2(p\text{-fum})_2]^{3+}$, 85661-85-4; $[Ru(bpy)_2(N\text{-Me-py})_2]^{4+}$, 85661-68-3; $[Ru(bpy)_2(N\text{-Me-py})_2]^{5+}$, 85661-86-5; $[Ru(phen)_2(vpy)_2](PF_6)_2$, 85717-44-8; $[Ru(phen)_2(vpy)_2](PF_6)_2$ (polymer), 85717-42-6; $[Ru(phen)_2(vpy)_2]^{3+}$, 85661-87-6; $[Ru(trpy)(stilb)_2Cl]PF_6$, 85661-56-9; $[Ru(trpy)(stilb)_2Cl]PF_6$ (polymer), 85661-44-5; $[Ru(trpy)(stilb)_2Cl]^{2+}$, 85661-88-7; $[Ru(i\text{-Pr-bpy})_2(p\text{-cinn})_2](PF_6)_2$, 85661-60-5; $[Ru(i\text{-Pr-bpy})_2(p\text{-cinn})_2]^{3+}$, 85661-89-8; $[Ru(trpy)(vpy)_3](PF_6)_2$, 85661-54-7; $[Ru(trpy)(vpy)_3](PF_6)_2$ (polymer), 85661-45-6; $[Ru(trpy)(vpy)_3]^{3+}$, 85661-90-1; $[Ru(trpy)(BPE)_3](PF_6)_2$, 85717-50-6; $[Ru(trpy)(BPE)_3](PF_6)_2$ (polymer), 85760-65-2; $[Ru(trpy)(BPE)_3]^{3+}$, 85661-91-2; $[Ru(trpy)(stilb)_3](PF_6)_2$, 85661-55-8; $[Ru(trpy)(stilb)_3](PF_6)_2$ (polymer), 85661-46-7; $[Ru(trpy)(stilb)_3]^{3+}$, 85661-92-3; $[Ru(trpy)(4'\text{-Cl-stilb})_3](PF_6)_2$, 85680-75-7; $[Ru(trpy)(4'\text{-Cl-stilb})_3](PF_6)_2$ (polymer), 85661-47-8; $[Ru(trpy)(4'\text{-Cl-stilb})_3]^{3+}$, 85661-93-4; $[Ru(HC(pz)_3)(vpy)_3](PF_6)_2$, 85661-57-0; $[Ru(HC(pz)_3)(vpy)_3]^{3+}$, 85661-94-5; $[Ru(trpy)(bpy)Cl]PF_6$, 83572-47-8; $Ru(phen)_2Cl_2$, 85718-09-8; *cis*-$Ru(bpy)_2Cl_2$, 19542-80-4; $Ru(trpy)Cl_3$, 72905-30-7; *cis*-$Os(bpy)_2(CO_3)$, 81831-23-4; *cis*-$Os(bpy)_2Cl_2$, 79982-56-2; *cis*-$[Ru(bpy)_2(N\text{-Me-cinn})_2](PF_6)_2$, 85661-49-0; $Ru(bpy)_2Cl_2$, 15746-57-3; $[Ru(bpy)_2(p\text{-}CH_2\text{-cinn})_2](PF_6)_2$·$[Os(bpy)_2(p\text{-cinn})_2](PF_6)_2$ (copolymer), 85718-08-7; $[Ru(bpy)_2(p\text{-cinn})_2](PF_6)_2$·$[Ru(i\text{-Pr-bpy})_2(p\text{-cinn})_2](PF_6)_2$ (copolymer), 85700-63-6; Pt, 7440-06-4; *p*-cinn, 85649-70-3; *p*-CH_2-cinn, 85649-71-4; *m*-cinn, 16054-96-9; *p*-fum, 85649-72-5; *N*-Me-cinn, 85649-82-7; *N*-Me-py, 85649-73-6; ferrocene derivative, 85661-62-7; oxidized ferrocene derivative, 85661-73-0; cinnamoyl chloride, 102-92-1; 4-aminopyridine, 504-24-5; fumaric acid, ethyl ester, 2459-05-4; β-(3-pyridyl)acrylic acid, 1126-74-5; β-(3-*N*-methylpyridyl)acrylic acid, 85649-69-0.